STUDY OF VIBRATION MEASUREMENT BY LASER METHODS

By Gail A. Massey

Prepared under Contract No. NAS2-3137 by
Electronic Defense Laboratories
SYLVANIA ELECTRONIC SYSTEMS
Mountain View, California

for

NATIONAL AERONAUTICS AND SPACE ADMINISTRATION

TABLE OF CONTENTS

LIST OF ILLUSTRATIONS

STUDY OF VIBRATION MEASUREMENT BY LASER METHODS

By Gail A. Massey
Sylvania Electronic Systems

SUMMARY

A four-month study of laser techniques for detecting and measuring vibrations of a spacecraft model on a shake table has been conducted. The range of vibration amplitudes considered is below one-half inch peak-to-peak and the frequencies are from 10 cps to 2000 cps. Eight different systems were considered. Three of these use microwave subcarrier amplitude modulation on the laser beam; vibrations of the reflecting surface are detected as phase shifts on the demodulated subcarrier signal. Two other systems use coherent optical detection in which phase shifts on the optical carrier are detected. Two spot projection techniques, in which the angular position or interference in the reflected light is used to indicate surface movement, were also studied. In addition, an interference mapping technique, similar to holography in some respects, was developed. It appears that the coherent detection systems may be useful in measuring vibrations down to one micron peak amplitude or perhaps less, even on diffusely reflecting surfaces. The microwave systems provide the poorest sensitivity. The interference mapping system gives a visual indication of surface tilt or gradient of normal displacement, and thus can provide a useful map of positions of maximum and minimum displacement. Most of the systems were tested experimentally; results were generally in good agreement with the analysis. This report contains a detailed description of each approach, a comparison of the relative performances of the various systems, and recommendations for further investigation and development of the most promising techniques.

INTRODUCTION

The purpose of this study has been to investigate methods of using the properties of laser radiation for detecting and measuring mechanical vibrations. The specific application that has been considered is the measurement of displacements on a spacecraft model which is vibrating on a shake table, although most of the techniques that have been considered are of interest for other uses, such as transducer calibration or precise distance measurement.

For purposes of system analysis, the detection and measurement problem has been defined as follows:

A. The vibrating object has an extended surface which may be irregular in shape. Optically the surface may be a specular or diffuse reflector, although the diffuse case is of primary interest because most surfaces will fall into this category. The peak-to-peak excursions of the moving surface may be as large as one-half inch, and the minimum deflections may be arbitrarily small. However, room vibrations and currents of warm or cold air moving through the optical path can produce time-varying uncertainties in the measurements up to a few microns at frequencies below 100 cps, implying a lower limit to the vibration amplitudes of the order of one micron. In addition to displacement measuring, it may be desirable to scan the surface to discover the points of maximum deflection.

B. The frequency range of the vibrations is 10 cps to 2000 cps. Since the spacecraft model is excited by a shake table, most of the vibration measurements will be made on surfaces whose motion is a sinusoid at a known frequency. Because the resonant frequencies of large mechanical structures are generally very low, the largest excursions would be expected at the lowest frequencies.

C. The laser system to be used should be reasonably small and portable. Elaborate cooling systems for the laser or optical detectors are to be avoided. Generally the system will be located close to the vibrating surface; the ranges of interest extend from a few inches to a few feet. The fact that this system is to be a measurement tool implies that reliability of operation, stability, and minimum maintenance are important considerations. These requirements essentially eliminate all cw laser sources except the helium-neon laser. Detector and modulation considerations, as well as simplicity of use, show that operation in the visible spectrum is preferable to the infrared. As a basis for comparative calculations, we have therefore taken the wavelength to be 6328Å. Two representative output power levels have been chosen. In the coherent detection systems, where single-frequency operation is desirable, the power level has been taken to be 0.1 milliwatt. For the other systems, the level is taken to be three milliwatts, which is readily obtained from commercially available units less than two feet long. The numerical calculations in the following sections are based on a worst-case condition of a diffusely reflecting surface placed three feet from an optical receiver with an aperture diameter of three inches.

In the section below, the systems which have been investigated are described. Calculations of sensitivity, description of the necessary components, and the results of experimental measurements are included in the discussion of each system. Schematic diagrams of each system, indicating the required components, are included. The last section contains a brief comparison of the performance of the various techniques, and those which are sufficiently promising to merit further development have been selected. Appendix A contains a detailed description of the operating principles and characteristics of the Sylvania microwave optical modulator. Appendices B and C are reprints of two papers concerned with laser spectral control. These techniques may ultimately be of practical interest for systems requiring large optical power levels for operation at greater distances.

DETECTION TECHNIQUES

A variety of methods are at hand for utilizing the frequency coherence, spatial coherence, or modulation capacity of laser light to measure the components of motion of a moving reflector. For the applications of interest to this study, the important components are excursions of a reflecting element normal to the surface and angular deflection or tilt of the reflecting element about some axis in the plane of the surface. Methods for detection of both types of motion have been analyzed and demonstrated.

In general the surface motion can be detected by observing its effect on the phase or frequency of a high-frequency subcarrier which has been amplitude modulated onto the optical carrier, or by observing the phase or frequency changes on the reflected optical carrier itself. In addition, the surface acts as a source of reflected light which changes its orientation in space with respect to the optical receiver; hence the angle of arrival of reflected light varies with target position and can be detected. All of the vibration measurement techniques that have been studied fit into these general classifications.

When the subcarrier methods are used, the vibration-induced phase shift is proportional to the ratio of the vibration amplitude to the subcarrier wavelength. Obviously then, it is desirable to use the highest possible subcarrier or modulation frequency at which efficient modulation and detection can be performed. Using the best state-of-the-art modulators and detectors, this frequency is in the microwave range near S-band. For this reason, the subcarrier techniques will be referred to as microwave systems.

When the optical carrier is used, a photodetector alone is not adequate to detect frequency changes as small as those produced in this application. Some type of optical interference is required to convert optical phase variations on the reflected signal into intensity variations (interference

fringes) which the photodevice can detect. A reference beam from the laser transmitter may be used to produce the interference with the incoming signal beam collected by the receiver optics. In such a system, the reference beam is often called the "local oscillator" beam, using the terminology established for radio frequency receivers. Demodulation using a reference beam is known as coherent detection. If the frequency of the reference or local oscillator beam is the same as the transmitted signal, the system is a coherent optical phase detector, or "homodyne" system. When the frequency of the reference is shifted with respect to the transmitted wavelength, an electrical beat is produced by the square-law photodetector at the difference, or intermediate, frequency between the two beams. Such a system is called a "heterodyne" detector or coherent optical intermediate frequency system. Obviously, the coherent phase detector or homodyne is a special case of heterodyne detection with the intermediate frequency (IF) equal to zero.

If the photodetector in the optical homodyne is replaced by an extended photographic plate of sufficiently high resolution and the receiver optics are removed, the interference fringes produced by the reflected light and reference beam can be recorded, provided the reflecting surface is nearly stationary during the exposure. Such a photographic recording is called a hologram, and the developed negative can be used to reconstruct a three-dimensional image of the surface. It should be emphasized that a reference beam is used in making the hologram. If the surface is a diffuse reflector, interference can take place even without a reference beam. This self-interference produces the well-known "sparkle patterns" which always appear in diffusely reflected laser light. These patterns are simply related to the surface position, and are the basis for the interference displacement mapping technique.

Microwave Subcarrier Systems

Three different microwave subcarrier systems have been analyzed. Each of them uses an electro-optic amplitude modulator to vary the intensity of the transmitted laser beam at a microwave rate. In practical devices, only a fraction, M, of the light intensity is modulated. These intensity variations represent a subcarrier envelope on the optical carrier; they can be detected by a photodetector which has good enough high frequency performance to respond to intensity variations at the subcarrier frequency. When the modulated light is reflected from the moving surface, the phase of the subcarrier envelope will vary with time according to the expression:

$$\phi(t) = \frac{4\pi x_0}{\lambda_m} \sin\omega_r t$$

where x_0 is the zero-to-peak vibration amplitude, ω_r is the vibration frequency, and λ_m is the microwave subcarrier wavelength. For a subcarrier frequency of 3 Gc/second, λ_m is 10 centimeters; thus the peak phase deviation for small vibrations is much less than one radian. The information about the vibration state of the surface appears on the reflected light in the subcarrier sidebands produced by the time-varying phase changes. For small peak phase deviations, which are always of interest in determining the maximum sensitivity of a given system, only the first two sidebands are significant (the exact expression gives an infinite set of sidebands with bessel function amplitudes, most of which are negligibly small). In that case, the reflected spectrum of light intensity is given by the approximation:

$$\begin{aligned} P = {} & \frac{P_0}{2} && \text{(unmodulated light)} \\ & + \frac{MP_0}{2} \sin\omega_m t && \text{(subcarrier)} \\ & + \frac{MP_0}{2} \frac{\pi x_0}{\lambda_m} \sin(\omega_m + \omega_r)t \\ & - \frac{MP_0}{2} \frac{\pi x_0}{\lambda_m} \sin(\omega_m - \omega_r)t \end{aligned} \quad \Big] \text{(sidebands)}$$

where ω_m is the microwave signal, M is the modulation index of the incident light, and P_0 is the reflected power. The necessary receiver bandwidth is simply the maximum range of vibration frequencies to be measured. Thus any usable microwave system must be able to detect the sideband amplitudes in the presence of receiver noise integrated over the required bandwidth. It should be noted that the above expression is for optical power; the demodulated power spectral components in the electrical circuits will be proportional to the squares of the individual terms in the equation above. This is important because signal-to-noise ratios are usually expressed as electrical quantities which are directly measurable.

The electrical noise power supplied by a photodetector into the first stage of the receiver amplifier can be represented by:

$$P_n = FkTB + 2eI_0B(n^2R_{eq})$$

where

- F = front end noise figure
- k = Boltzmann's constant
- T = absolute temperature
- B = receiver bandwidth
- e = electron charge
- I_0 = average photocurrent from all powers
- n = current multiplication, if any, in the detector
- R_{eq} = equivalent detector output impedance.

The first term above is unavoidable, but the second, or shot noise component, is determined by dark current in the detector plus the optical signal-induced photocurrent. In detectors without multiplication, such as semiconductor diodes, the thermal noise will predominate at low light levels. For large light levels, or for substantial multiplication factors, the shot noise may be larger. Often detectors are rated by their noise equivalent power (NEP), which is the minimum detectable optical input for a given detector and bandwidth.

The other characteristic of interest for a given photodetector is its response to an optical signal. Photodetectors are square-law devices; that is, the photocurrent I is linearly related to the input optical power P:

$$I = SP = \frac{n e}{h\nu} P$$

Here S is the response of the detector in amperes per watt, η is the quantum efficiency, h is Planck's constant, and ν is the optical frequency. The electrical signal power out of the detector is given by:

$$P_s = 1/2 i_s^2 (n^2 R_{eq})$$

where i_s is the peak photocurrent induced by an alternating optical input signal power.

From the relations above, the performance of the various systems can easily be evaluated.

Direct Phase Detection System. - This approach is the simplest microwave technique and has been demonstrated experimentally during this program. The system is shown schematically in Figure 1. The subcarrier is recovered after reflection by the photodetector, which might be a tube or solid state diode. The diode has the disadvantages of no multiplication and effective output impedances of only a few hundred ohms at best. However, solid state quantum efficiencies can approach unity. For comparison, the Sylvania multiplier-traveling-wave phototube has a $(n^2 R_{eq})$ product of 6×10^9 ohms, representing a large current multiplication, with a photocathode quantum efficiency about 10^{-3}. Since the figure of merit is $\eta^2 (n^2 R_{eq})$, the present tube is somewhat better than the best diode. Development of different photocathodes than the presently available S-1 type is possible; thus it is likely that tube performance will continue to improve. The tube

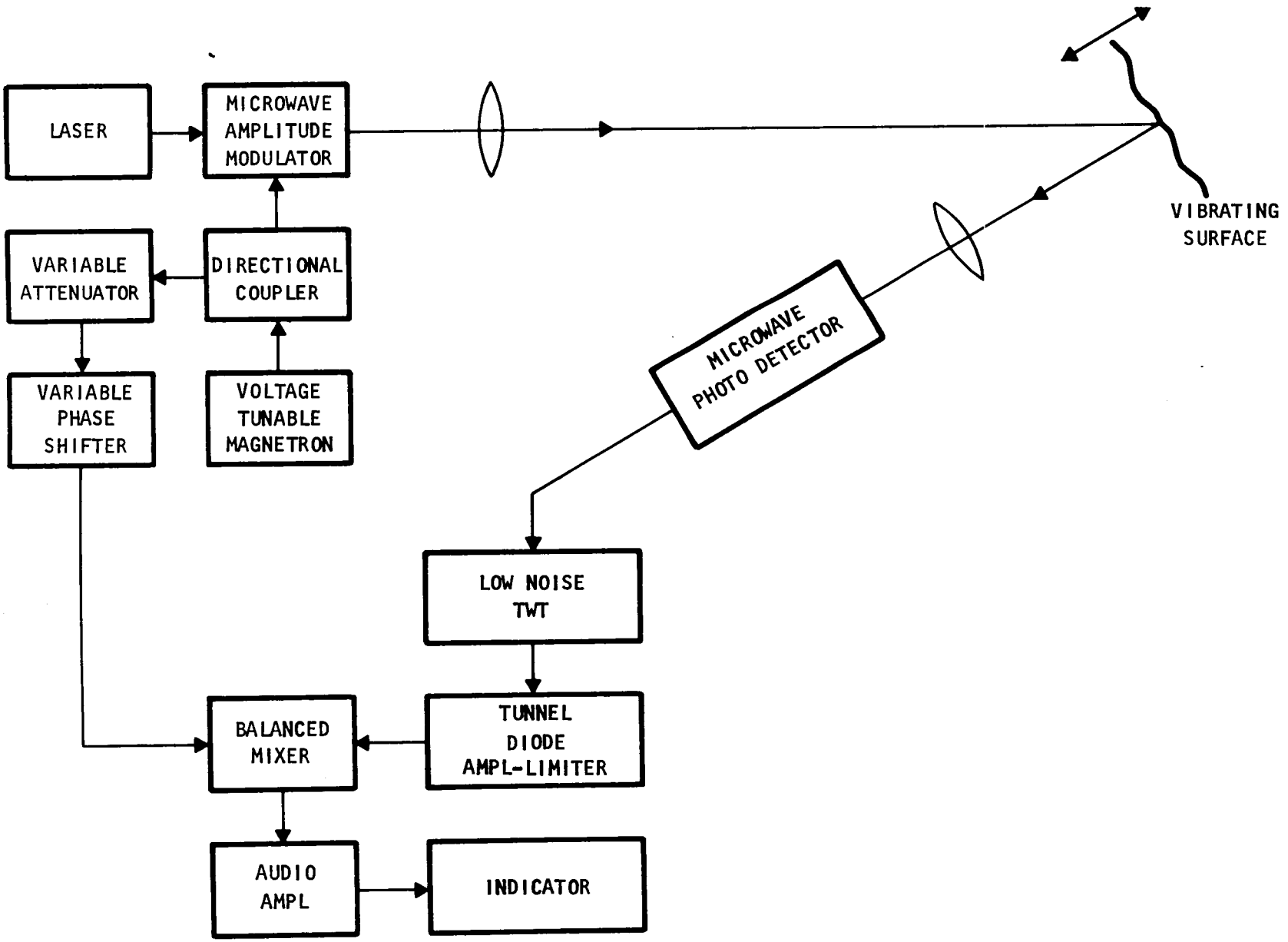

Figure 1. Microwave Direct Phase Detection System.

was used in this study both as a basis for calculations and as a part of the experimental work.

The low-noise traveling-wave amplifier and tunnel diode limiter are required to suppress low-frequency amplitude fluctuations on the received signal due to surface tilt, laser amplitude fluctuations, and other effects. The balanced mixer further rejects amplitude modulation on either of the microwave input signals.

The voltage tunable magnetron was chosen as the microwave exciter for the optical modulator. The modulator power requirement is between one and two watts cw. This might be tuned by a servo-control system, not shown in Figure 1, to follow the 20 Mc/sec drift in modulator resonant frequency during warmup. Such a servo-system would include a sensor placed in or near the modulator cavity to sample the phase and amplitude of the cavity field. This signal would be processed by narrow-band electronics to derive the tuning voltage needed to make the oscillator track the cavity resonance. No attempt was made during this study to construct such a control system, but this could be done if manual tracking of the generator is undesirable.

The directional coupler, attenuator, and variable phase shifter provide the reference or local oscillator signal to the balanced mixer at the proper phase and amplitude for phase quadrature detection. The required local oscillator power level is about 10 milliwatts into the mixer. It has been found experimentally that the phase adjustment can be set simply by maximizing the output audio signal while measuring a surface vibration of constant amplitude.

Mixing the microwave signals directly to an audio difference degrades the mixer noise figure to about 10 db. This does not affect performance of the present system because considerable amplification and dynamic range compression precedes the mixer stage in the signal channel. Even without

the excess (shot) noise from the photodetector, the microwave noise figure would be determined by the traveling-wave amplifier at the front end. As will be shown below, the microwave components function essentially as an ideal receiver, and limitations to this system are imposed by optical considerations.

Using the sideband analysis above, and the expressions for detector output signal and noise, the detection signal-to-noise ratio is seen to be:

$$\frac{S}{N} = \frac{\frac{1}{2}\left(\frac{ne}{h\nu}\right)^2\left(\frac{\pi\rho M P_0 K_r x_0}{\lambda_m}\right)^2 (n^2 R_{eq})}{FkTB + 2eB\,\frac{ne}{h\nu}\,\frac{\rho P_0 K_r}{2}\,(n^2 R_{eq})}$$

Here P_0 is the laser output power, ρ is the surface reflectance, and K_r is the geometrical fraction of the transmitted light reflected into the receiver. For specular surfaces K_r might equal unity, but for diffuse reflectors K_r is given by:

$$K_r = \frac{d^2 \cos\theta}{4D^2}$$

where d is the receiver diameter, D is the distance from receiver to surface, and θ is the angle the receiver makes with respect to the surface normal (usually $\cos\theta$ is approximately unity).

By setting S/N = 1 we can solve for the minimum detectable vibration amplitude x_0, which is:

$$x_0(\min) = \frac{\left[2FkTB + 2eB\,\frac{ne}{h\nu}\,(\rho P_0 K_r)(n^2 R_{eq})\right]^{\frac{1}{2}}}{\frac{ne}{h\nu}\,\frac{\pi\rho M P_0 K_r}{\lambda_m}\,(n^2 R_{eq})^{\frac{1}{2}}}$$

If we choose the typical values for the various parameters given below, we can obtain a numerical sensitivity.

Let:

P_0 = 3 milliwatts

M = 0.1

B = 10^4 cps

kT = 4.1×10^{-21} joule

F = 3

λ_m = 10 centimeters

η = 6×10^{-4} electrons per photon

$e/h\nu$ = 0.5 coulomb per joule (wavelength = 6328Å)

K_r = 1.7×10^{-3} (diffuse reflector)

ρ = 0.1

n^2R_{eq} = 10^9 ohms.

Then from the above, $x_0(\text{min})$ for the microwave direct phase detection system is 1.8 millimeters. Such a large excursion could easily be detected by the unaided eye; thus it is unlikely that this system would be practical at such a bandwidth for measuring diffusely reflecting surfaces.

The experimental setup used in the tests differed from this analytical model only in that the surface was an aluminized mirror. The measured carrier-to-noise ratio was about 30 db using a spectrum analyzer receiver with B = 10^4 cps. When the mixer and audio stages were employed, and the microwave phase was properly adjusted, vibrations of one millimeter were readily measured using a tunable voltmeter and were clearly audible in a monitor headset. It was found that the limiter was essential to the elimination of large spurious AM signals due to surface tilt. To summarize, the system behaved as expected with the specular surface, with usable sensitivities down to a few thousandths of an inch or less.

Intermediate Frequency Detection System. - This technique is illustrated schematically in Figure 2. The receiver portion of this system differs from the one above because the local oscillator signal to the microwave mixer has been shifted in frequency by approximately 160 Mc/sec. This is the purpose of the intermediate frequency (IF) generator and sideband filter. The microwave mixer produces a beat frequency near 160 Mc when a signal is present. A second mixer, known as a phase detector, is used to demodulate the phase modulation produced on the IF by the surface motion. Thus the mixing down to audio is done in two steps. This improves the mixer noise figures, and with limiting in the IF amplifier it might be possible to operate the phototube directly into the first mixer. As pointed out in the previous section, the mixer noise is negligible anyway, so that the additional complexity of this approach appears unnecessary.

Sensitivity is the same as for the Direct Microwave Phase Detector analyzed above.

Double Modulation System. - The fundamental limitation in performance of the systems above is imposed by the low quantum efficiency of the microwave phototube. A method which avoids this problem has been analyzed and tested experimentally. It is illustrated in Figure 3. Here the phase demodulation is done not with a high frequency detector but with a gated receiver and low frequency detector. Gating of the microwave rate is accomplished by passing the reflected light back through the microwave optical modulator. A partial mirror or calcite prism and quarter-wave plate might be used to allow transmission and reception through the same optical system. The remodulated signal in this case will have audio frequency intensity variations corresponding to the subcarrier phase shifts produced by the vibration. Efficient, low noise phototubes and diodes are available at these frequencies.

With the external optical path adjusted so that the second modulation occurs 90° out of phase with the first one, the detected optical power is

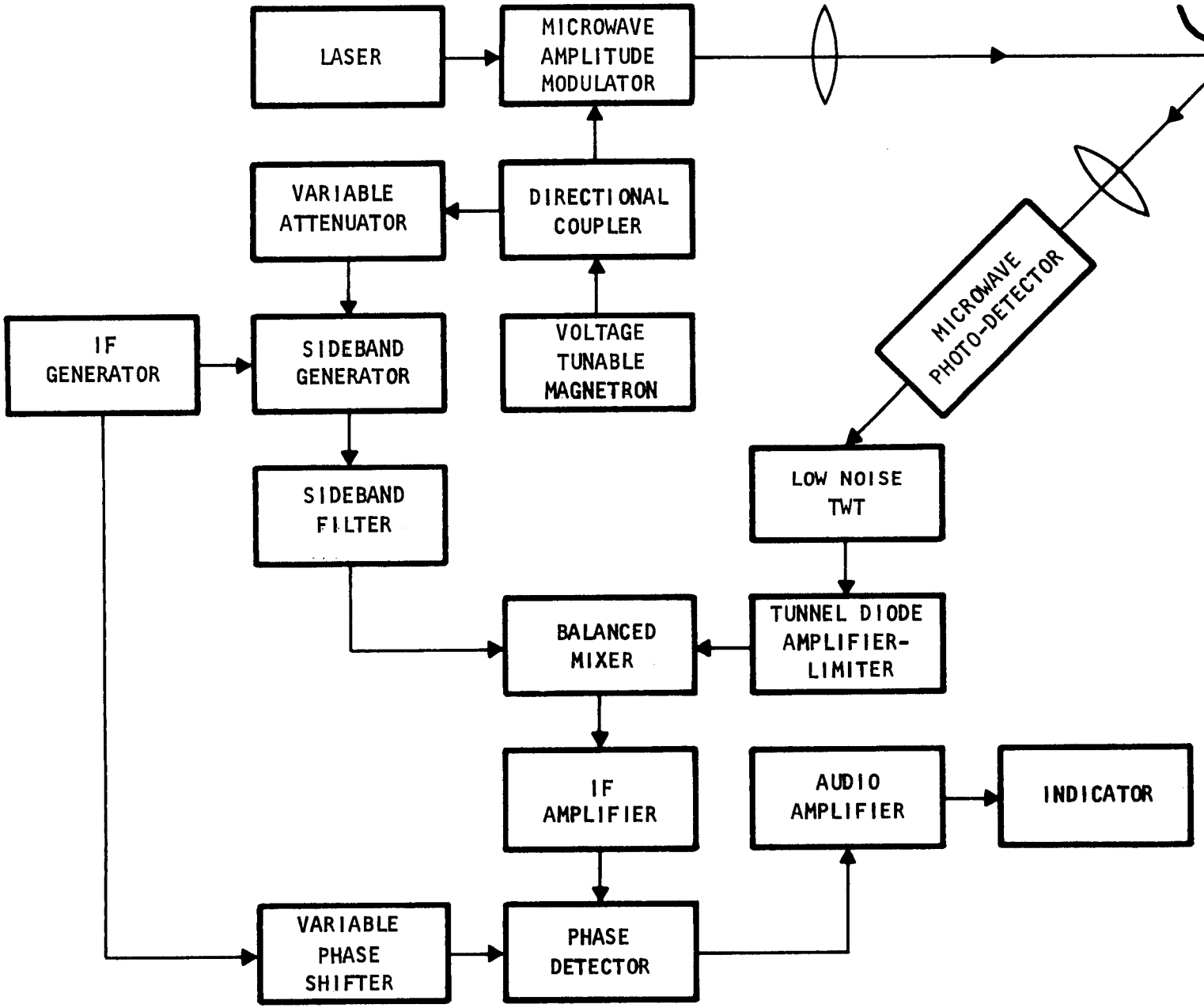

Figure 2. Microwave Intermediate Frequency Detection System.

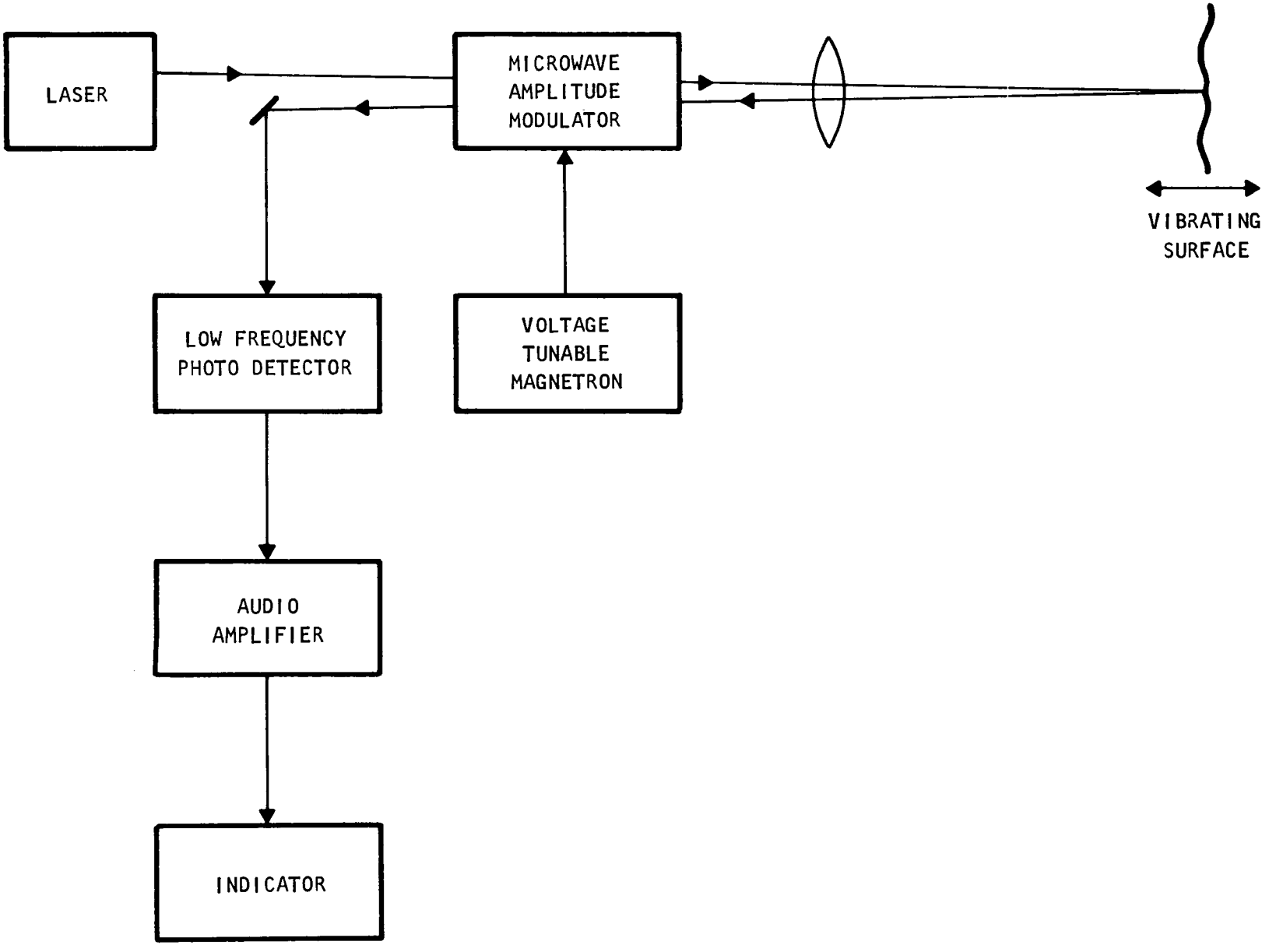

Figure 3. Microwave Double Modulation System.

of the form:

$$P = P_r\left[1 + M^2 \frac{2\pi x_0}{\lambda_m} \sin\omega_v t\right]$$

where P_r is the average power reaching the photodetector. At these frequencies detector noise is specified by NEP, which may be 10^{-9} watts for a silicon diode and 10^{-11} watts for a very good (S-20) multiplier phototube. Substituting NEP for the thermal noise in the signal-to-noise expression, we have:

$$\frac{S}{N} = \frac{\left[2\pi M \frac{x_0}{\lambda_m} K_r \rho P_0 S\right]^{\frac{1}{2}}}{4e\, K_r P_0 SB + 2(NEP)^2 S^2}$$

where S is the detector response in amperes per watt.

Solving for the minimum x_0:

$$x_0(\min) = \frac{\lambda_m\left[4e\rho K_r P_0 SB + 2(NEP)^2 S^2\right]^{\frac{1}{2}}}{2\pi M K_r \rho P_0 S}$$

Taking $S = 0.025$ amperes/watt for the tube and 0.25 amperes/watt for the diode, a calculation shows that the tube is shot noise limited and $x_0(\min) = 0.11$ millimeters using the same choice of parameters as for the other microwave systems. For the diode the (NEP) term is dominant, and the minimum measurable displacement is about ½ millimeter. This is somewhat better than the expected sensitivities of the other subcarrier systems.

Tests of this detection system were made in the laboratory, both at 1.5 Gc and at 2.4 Gc. Two frequencies were tried because the modulation index available at L-band is about 50% larger than at S-band. The tests revealed an important defect in this system which had been

suspected from the analytical results also. It was not possible to detect the phase shift on the subcarrier because of the large spurious amplitude fluctuations due to surface tilt. This was true even when the vibrating mirror was placed at the focal point of a lens, an optical geometry which minimizes the angular sensitivity. There are two fundamental reasons for this problem. From the expression given above for the subcarrier demodulated optical power, it is apparent that the modulated portion of the light reaching the detector is a very small fraction of the total level, since M^2 is about 10^{-2}. Thus any substantial amplitude change due to laser noise or reflected beam deflection will overcome the desired signal. The second reason is that the subcarrier demodulation to audio is done optically; thus it is not possible to use limiting to remove the large amplitude variations before detection. For this reason it is doubtful that this system could be used to its theoretical limit of performance even if the modulator were improved to make M almost unity. If this problem could somehow be eliminated, the double-modulation system would realize the advantage of requiring no microwave receiver components and could make use of the best possible optical detectors.

Coherent Optical Detection Methods

The vibration-induced phase shifts on the optical carrier can be coherently demodulated by combining the signal beam with a local oscillator beam which acts as a phase reference. When both beams are properly aligned and are incident on an optical detector, the output current is proportional to the square of the total incident electric field. This current may be written:

$$i(t) = I_{LO} + I_{SIG} + 2\sqrt{I_{LO}\, I_{SIG}}\, \cos(\omega_{LO}t - \omega_{SIG}t + \phi_{LO} - \phi_{SIG})$$

where I_{LO} is the direct current that would be produced by the optical

local oscillator field only, I_{SIG} is the direct current due to signal alone, ω_{LO} and ϕ_{LO} are the frequency and phase of the local oscillator, and ω_{SIG} and ϕ_{SIG} are frequency and phase for the signal wave. Clearly the first two terms represent the average current level, which contributes only shot noise in the frequency range of interest. The cosine term, whose rms value is $\sqrt{2\, I_{LO}\, I_{SIG}}$, is the beat frequency output and represents the heterodyne or homodyne signal. Ordinarily the local oscillator current is much larger than the signal, so that shot noise from the LO current is the dominant receiver noise. As I_{LO} is increased the beat frequency amplitude and the shot noise current $\sqrt{2eI_{LO}B}$ increase together. Thus for large I_{LO}:

$$\frac{S}{N} = \frac{2I_{LO}I_{SIG}}{2eI_{LO}B} = \frac{I_{SIG}}{eB}$$

This represents ideal receiver performance. Relating I_{SIG} to the optical signal input power P_{SIG} gives

$$I_{SIG} = \eta \frac{e}{h\nu} P_{SIG}$$

$$\text{or} \quad S/N = \eta \frac{P_{SIG}}{h\nu B}$$

The minimum detectable power is found by letting S/N = 1:

$$P_{SIG}(\text{min}) = \frac{1}{\eta} h\nu B$$

For an ideal detector with $\eta = 1$ at 6328Å with $B = 10^4$ cps:

$$P_{SIG}(\text{min}) = 3.2 \times 10^{-19} \times 10^4 = 3.2 \times 10^{-15} \text{ watts.}$$

This very small power level indicates the sensitivity of coherent detection. It should also be noted that a total surface motion of only 1/2 optical wavelength changes the optical phase, and thus the

beat frequency phase, by 2π radians. This represents a large phase modulation; hence the minimum power derived above is also approximately the minimum that is required to allow measurement of deflections as small as 3200Å, or 3.2×10^{-5} centimeters. For large displacements ϕ_{SIG} changes through many cycles away from its average value because of the large Doppler shift on the reflected light. The maximum shift is given by

$$\Delta f = \frac{2x_0\omega_r}{\lambda_0} = 4\pi f_r \frac{x_0}{\lambda_0}$$

for a sinusoidal vibration of peak amplitude x_0, frequency f_r, measured with laser radiation of wavelength λ_0. If the maximum peak-to-peak excursion is 1/2 inch at 10 cps, the maximum Doppler shift away from the average beat frequency is approximately 1.3 megacycles per second. Thus the detector must have good enough frequency response to provide a 1.3 Mc bandwidth if $\omega_{LO} = \omega_{SIG}$, or a bandwidth of 2.6 Mc if $(\omega_{LO} - \omega_{SIG})$ is adjusted to produce an intermediate frequency beat well above 1.3 Mc. Ample frequency response for either case is provided by all conventional multiplier phototubes and some photodiodes. Since relatively small local oscillator powers are required for ideal shot-noise-limited operation in multiplier phototubes, and because the dynode structure in such devices provides high gain with uniform frequency response, the tubes may be preferable to the diodes, even though $\eta = 0.05$ for an S-20 cathode and $\eta = 0.5$ for a good silicon diode.

For deflections much less than λ_0 an analysis similar to that used in the microwave subcarrier cases can be applied. The fraction of power in the phase-modulated sidebands must be greater than the noise. If the phase or frequency of the local oscillator beam is adjusted so as to permit demodulation of these sidebands, then:

$$x_0(\text{min}) = \frac{\lambda_0}{2\pi} (S/N)^{-\frac{1}{2}}$$

where (S/N) is the signal to noise ratio for the unmodulated carrier, or

$$x_0(\text{min}) = \frac{\lambda_0}{2\pi} \left(\frac{h\nu B}{\eta P_{SIG}}\right)^{\frac{1}{2}}$$

Since all of this analysis is based on a single-frequency laser, the effects of operation in several frequencies, which is often the case for moderate and high power lasers, have to be included in addition. The primary effect is to produce overlapping beat components at the IF frequency, one for each laser mode. The phase of each component depends on the optical path to the surface, and since the modes differ in frequency by 100 to 500 Mc/sec, the overlapping beat components change in relative phase with every few inches of additional optical pathlength. The result is that the observed net beat signal is small for most distances but periodically becomes as large as if the laser were actually monochromatic. These multiple locations of the surface for maximum signal are spaced exactly one laser cavity-length apart. The surface must be within a few inches of one of these positions to produce the optimum signal.

In addition, a multi-frequency laser may have noise on the output because the oscillating frequencies are not exactly evenly spaced and have random relative phases. This noise, present on the local oscillator beam, can seriously degrade the coherent receiver sensitivity.

For this application, with small distances to the surface, it would seem desirable to use a commercial single-frequency laser with low output power, rather than to resort to laser spectral control methods to avoid the problems above. Power outputs of 0.1 milliwatts can be obtained in a single frequency using available devices. With such a laser and the usual three-inch optics and three-foot surface distance, it is reasonable

to expect P_{SIG} to be about 10^{-8} watts. Then using an S-20 phototube and filter with an effective η of 10^{-2}, we have:

$$x_0(\text{min}) = 5.7 \times 10^{-8} \text{ centimeters.}$$

In a practical case, ambient vibrations of the laser and optical components, as well as air currents in the path and surface interference effects, will probably degrade the minimum value considerably, so that $x_0(\text{min})$ approximately equal to 10^{-4} centimeters would appear to be a more realizable estimate of the sensitivity.

Coherent Optical Phase Detection System. - If the vibrations of the surface are approximately sinusoidal and larger than an optical wavelength, it should be possible to use coherent homodyne detection with the local oscillator frequency the same as the average signal frequency. This phase detection system is essentially a Michelson interferometer with a gated counter following the photodetector. It is shown schematically in Figure 4. The output optical system is used to focus the transmitted light to a point on the surface, a necessary condition for efficient photomixing. All of the optical components which process the signal and local oscillator beams separately must be free from aberrations to well below the diffraction limit; otherwise some portions of the mixing wavefronts will be out of phase and cancel. The angular tolerance on the alignment of the partial mirror is less than the ratio of the optical wavelength to the beam diameter at the mirror. For a practical system this would be a fraction of a milliradian.

Since amplitude modulation will ordinarily be present on the reflected light, and therefore on the detector output, it will be necessary to have a limiting circuit in the counter. Distortion components from the limiting will fall in the frequency bands ordinarily occupied by Doppler components from larger velocities. Thus the counter must be digital (counting zero crossings) rather than analog (using tuned filters). Thus the maximum

beat frequency determines the final receiver bandwidth, since the trigger circuit in the counter must not count noise. This degrades the signal to noise ratio about 30 db below the theoretical maximum for this system. However, the great sensitivity of coherent detection is sufficient to make the system usable even with this drawback. The counter must be gated to count only the zero crossings during a known number of vibration cycles. This could be done using a reference signal from the shake table or in the counter using a detector indicating times of zero beat.

This system was set up in the laboratory. Tests were made using an aluminized mirror surface on the vibrator and a spectrum analyzer and oscilloscope in place of the counter. The system worked essentially as expected. Photographs of the photodetector output waveforms (without limiting) are shown in Figure 5. Deflections of approximately 10^{-4} centimeters were easily measured using the oscilloscope as a display, and much larger values could be estimated from the spread of the sidebands on the spectrum analyzer. No serious problems with frequency stability of the laser or isolation of the reflected light from the moving mirror were noticed during the experiments.

Coherent Intermediate Frequency Detection System. - With present techniques it is possible to translate a substantial fraction of the laser optical carrier to a new optical frequency which differs from the original by a radio frequency difference. This may be done by various sideband-cancelling modulation techniques or by diffraction from acoustic waves. For use as a local oscillator in a coherent heterodyne receiver, it is important to have the shifted frequency free from spurious modulations which could interfere with the normal operation of the receiver circuitry. Since practical optical filters are not available with sufficiently narrow bandwidths to isolate the optical sidebands due to radio frequency modulation of the laser, it is difficult to get adequate spectral purity using the modulation techniques mentioned

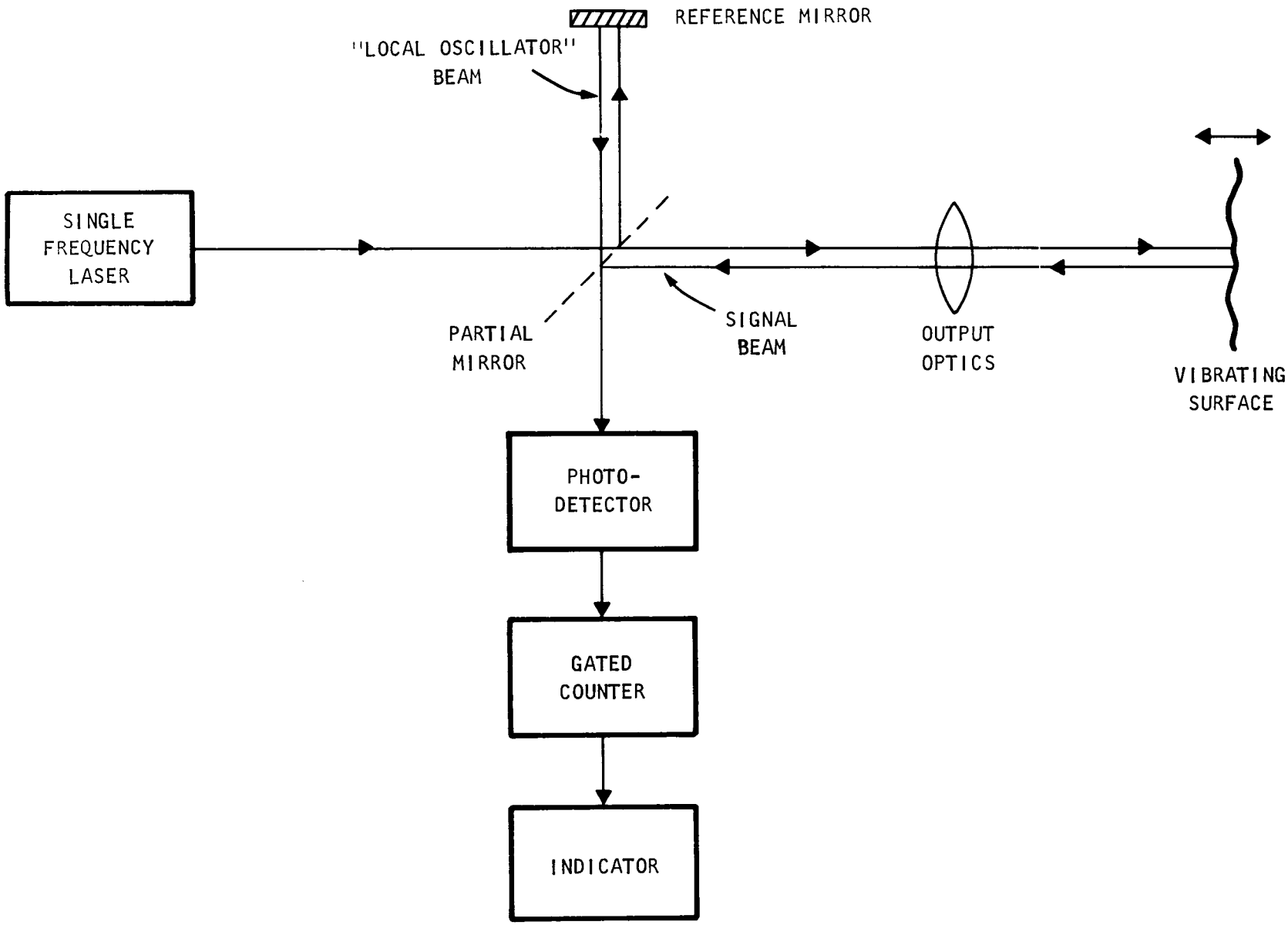

Figure 4. Coherent Optical Phase Detection System.

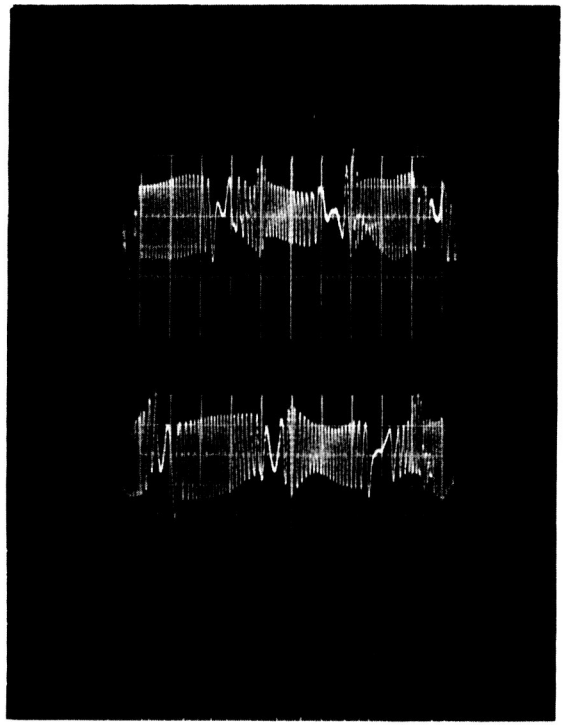

(a)

Vibration amplitude $x_0 = 10\lambda$ at 100 cps. Amplitude variations indicate the need for limiting in the receiver.

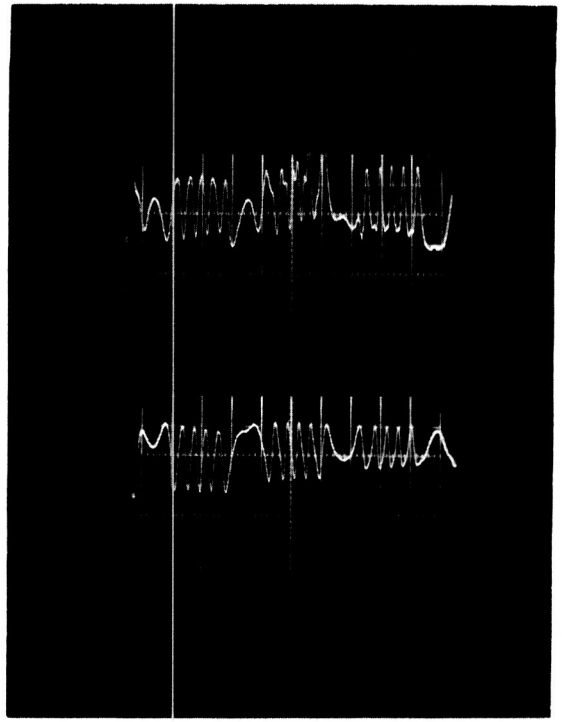

(b)

$x_0 = 2.5\lambda$ at 1000 cps.

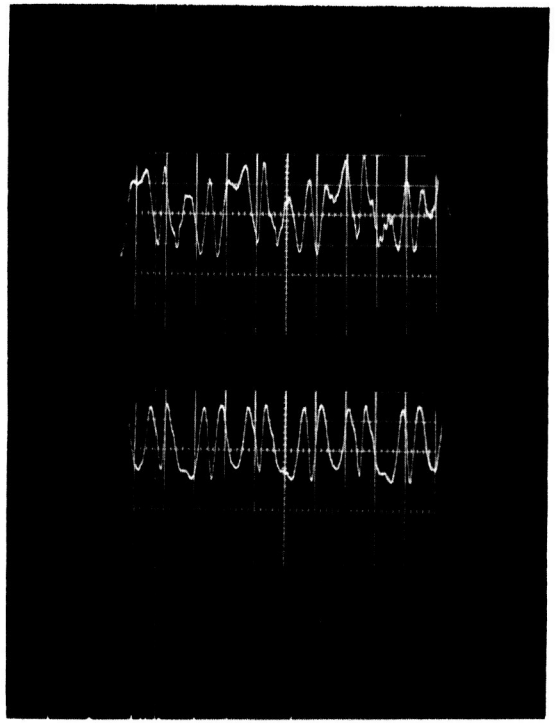

(c)

$x_0 = \lambda$ at 2500 cps. Method begins to fail at this level for x_0, due to ambient vibration (note upper trace).

Figure 5. Waveforms Obtained by Coherent Phase Detection.

above. However, the diffraction approach causes spatial separation of the sidebands; thus overlapping frequencies which constitute modulation can be avoided and the carrier-sideband separation is useful in practical optical systems. The acoustic diffraction technique has been selected for use in the present application.

The diffraction frequency translator, or Bragg cell, consists of a tank of water in which a radio-frequency traveling acoustic wave is generated by a large quartz transducer. Light entering the cell is diffracted by the density variations at the moving acoustic wavefronts, and several light beams, or diffraction orders, are usually present in the output. The undiffracted beam remains at the original frequency and is known as the zero order component. If the acoustic wave is a few centimeters wide and the input power is about one watt, an angle can be found where most of the light is in the zero and first orders, in equal proportions. This requires careful adjustment of the angle between the acoustic wave and the optical wave; when that condition is met, the shift in frequency of the first order beam is given by the Doppler shift on the light reflected from a mirror moving at the speed of sound in the direction of the acoustic wave. Because of a constraint between diffraction angle and acoustic frequency, the Doppler component is found to be exactly equal to the acoustic frequency for first order diffraction. Constraints imposed by the optical wavelength and acoustic attenuation limit the useful range of frequency shifts obtainable in this way to the 5-50 Mc/second band. Optimum performance is near 15 Mc/second, a convenient frequency at which to obtain large quartz transducers.

An intermediate frequency of 15 Mc/second is also convenient for the present application, since the expected maximum Doppler shift due to surface motion is a few megacycles per second. A diagram of a coherent intermediate frequency system using the Bragg cell is shown in Figure 6. The same close tolerances on the optics and mirror alignment as in the Coherent Optical Phase Detection System apply, but in this case a

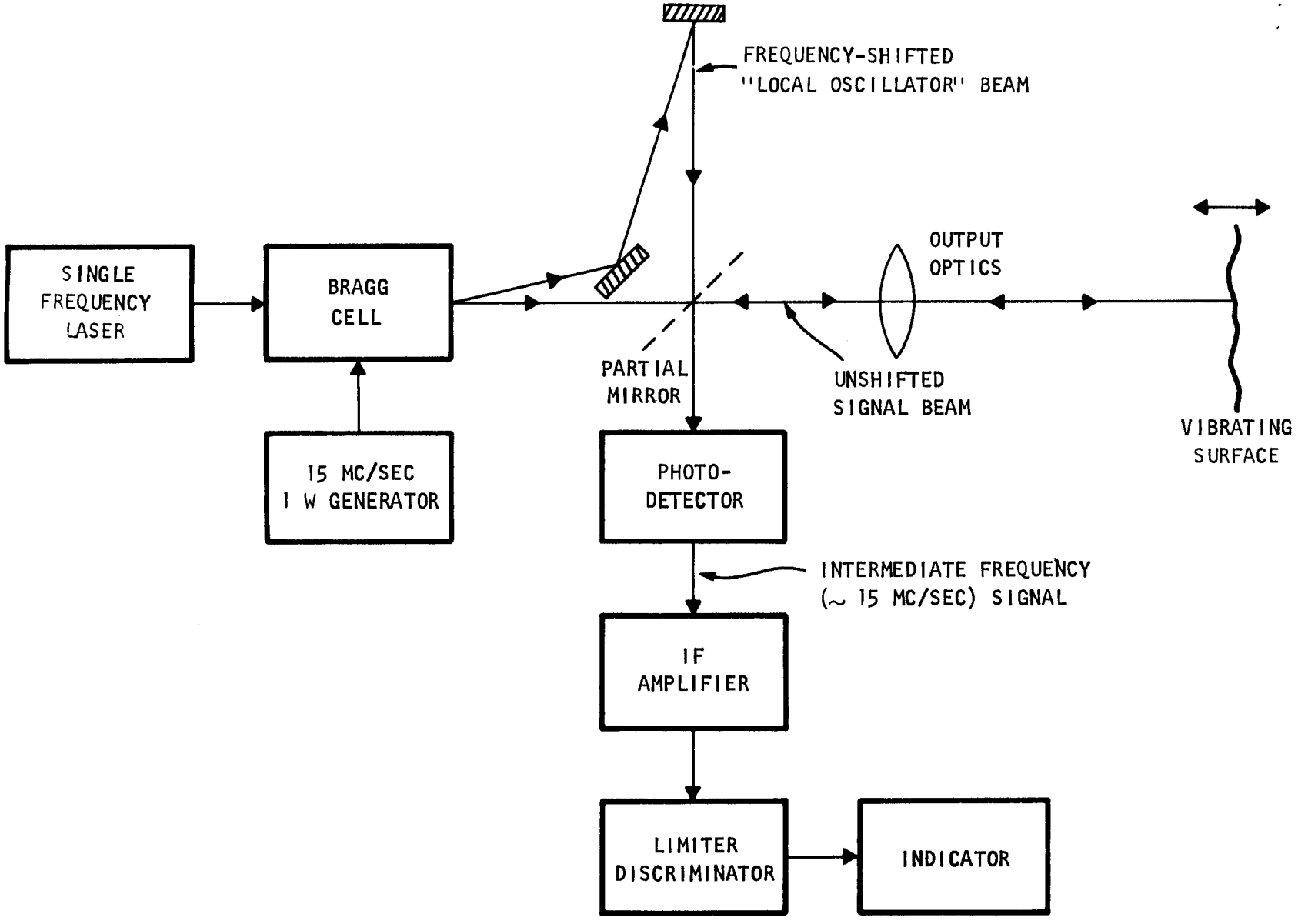

Figure 6. Coherent Intermediate Frequency Detection System.

discriminator can be used because the limiter-induced distortion products are at least 15 Mc from the center of the passband and can be filtered out. The post-detection system bandwidth can therefore be as small as audio, although it is still necessary to have sufficient signal to operate the limiter above the wideband pre-detection noise. If a multiplier phototube is used, much of the IF amplification is done in the tube and the circuit noise figure does not affect performance. If a frequency discriminator is used, it must be followed by an audio circuit which integrates those frequencies above the lowest vibration frequency, so that the high frequency emphasis of the discriminator will be removed at the output.

The optical components of this system were tested during the study. Results were very promising; a heterodyne signal was observed on the RF spectrum analyzer receiver for both specular and diffuse surfaces, at vibration amplitudes up to 1/4 inch. A single-frequency Spectra-Physics Model 119 laser with 0.1 milliwatts output was used, and the photodetector was an RCA 7265 tube with an S-20 cathode. Photographs of the spectrum analyzer display are shown in Figure 7.

In these tests the expected signal fluctuations due to surface interference were clearly observed; often the signal dropped more than 20 db during a fraction of the vibration cycle. Thus limiting would be needed in any coherent system working with diffuse reflectors.

Overall sensitivity obtained with this method was better than that of any other system tested during the study. In spite of the fact that many of the concepts and components used in this approach are new, it should be possible to reduce them to engineering practice in a system with reasonable size and power requirements.

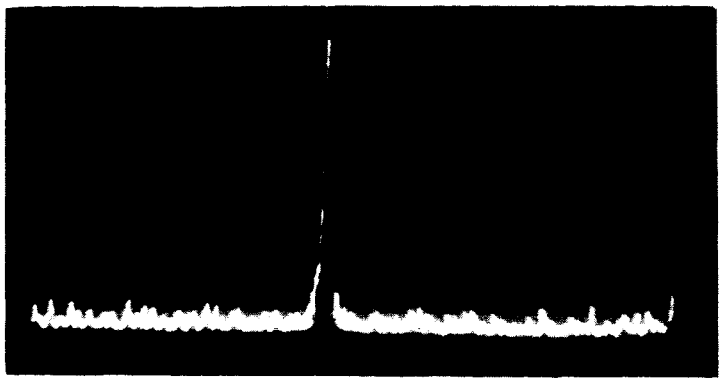

(a) 15 Mc/sec intermediate frequency detector output. Vibration amplitude $x_0 = 0$.

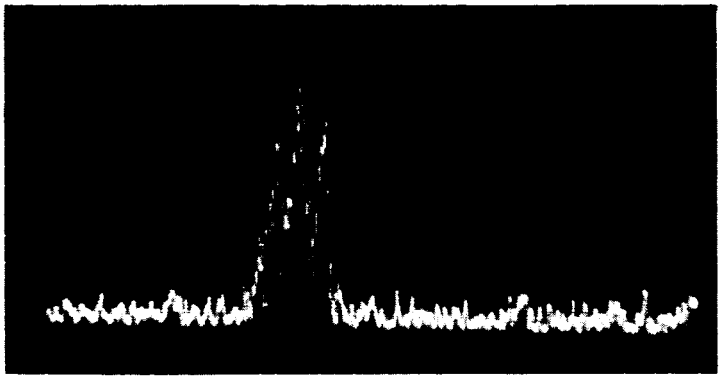

(b) Effect of laser noise on beat spectrum. Frequency spread about 50 kc/sec. A multimode laser was used here.

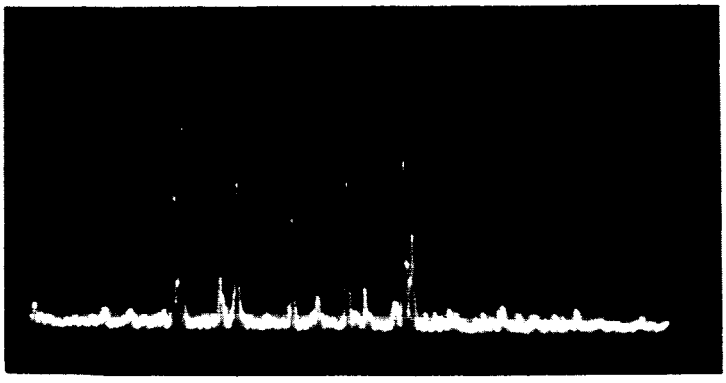

(c) Doppler spectrum with $x_0 \approx 24\lambda$ at 400 cps. Frequency spread is approximately 120 kc/sec. (Not all sidebands appear because of the rapid sweep of the RF spectrum analyzer.)

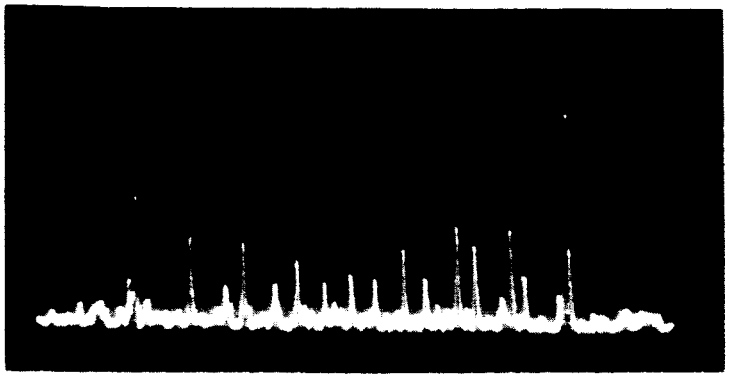

(d) Doppler spectrum with $x_0 \approx 40\lambda$ at 400 cps. Sideband spread is approximately 200 kc/sec.

Figure 7. Doppler Spectra Obtained with Coherent Intermediate Frequency Detection.

Spot Projection Systems

If the moving surface is a diffuse reflector, it is possible to obtain information about some components of the motion by projecting one or more spots of laser light onto the surface and measuring the motion-induced effects on reflected light collected by an optical receiver. One method, in which the apparent motion of the spot is measured, does not make use of the spectral coherence of the laser. This system has been called the incoherent spot projection technique. Another approach, in which two spots are projected and the interference between reflected waves from both of them is used, is known as coherent spot projection, because the laser coherence is utilized.

Incoherent Spot Projection System. - This system is illustrated in Figure 8. The laser beam is projected to a small spot on the vibrating surface. Some of the reflected light is collected by a rectangular receiver aperture. In the receiver focal plane, motion of the surface produces a lateral motion of the spot image. If a knife-edge stop is placed a short distance behind the image, where the beam has expanded to a rectangle, motion of the image affects the fraction of the light that passes the stop. In practice the stop would cover half the beam on the average, and the distance behind focus would be adjusted to accommodate the largest expected image displacements in the linear range. The fraction of power passing the knife-edge is measured by a photodetector whose current output is a linear analog of the surface displacement along the axis of the transmitted beam.

The dynamic range of measurable vibration is just the ratio of the average photocurrent to noise current in the detector. This is also the ratio of the maximum expected vibration to the minimum measurable vibration amplitude. Therefore:

$$\frac{i_n}{I} = \frac{P_n}{P_r} = \frac{x_0(\text{min})}{x_0(\text{max})}$$

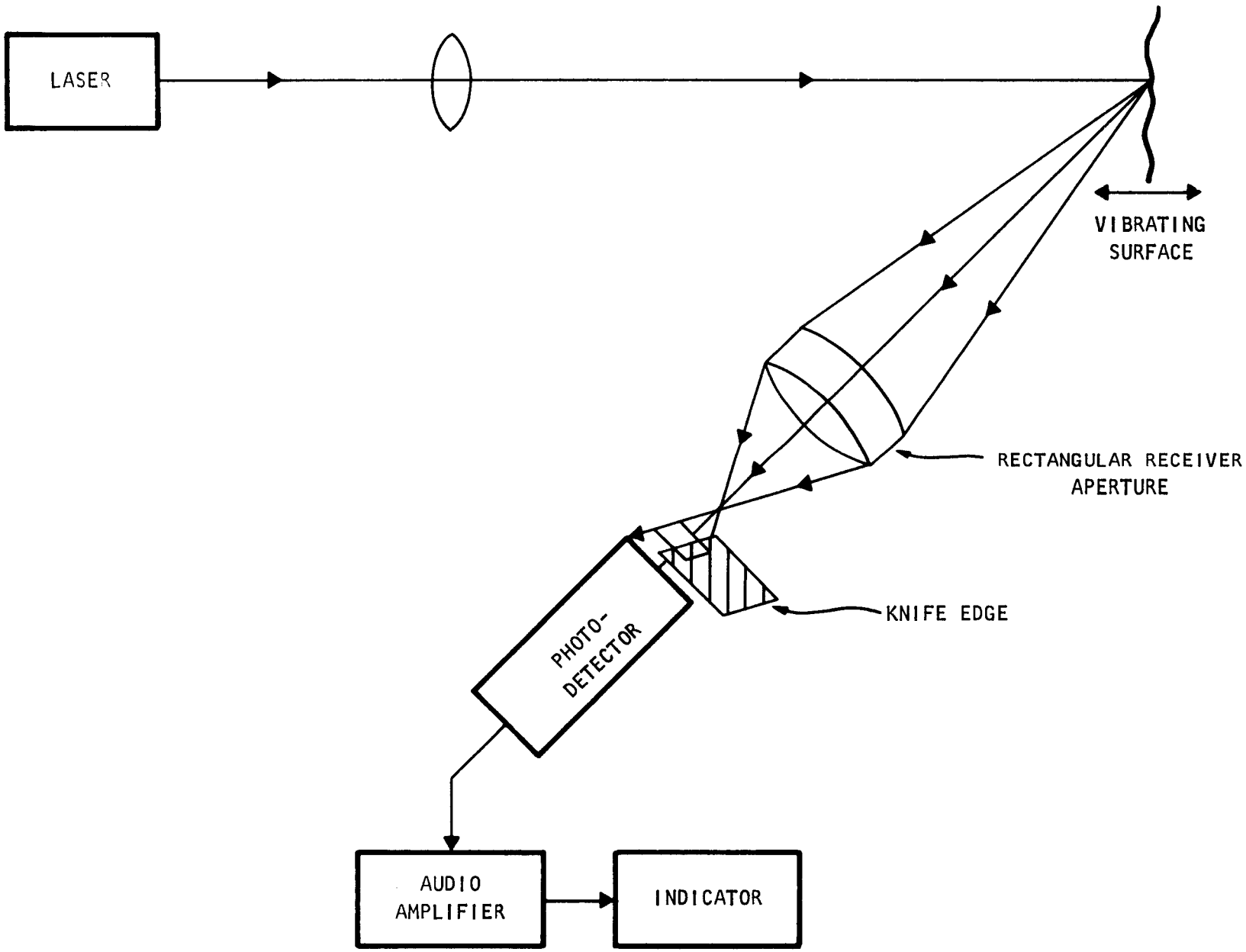

Figure 8. Incoherent Spot Projection.

where i_n, the noise current, corresponds to the optical power P_n, and I, the average photocurrent due to reflected light, corresponds to the received optical power P_r.

For the usual geometry and a three-milliwatt transmitter, a phototube can be shot noise limited. Then:

$$\frac{x_0(\text{min})}{x_0(\text{max})} = \sqrt{\frac{2h\nu B}{\eta P_r}}$$

For $x_0(\text{max})$ = 1/4 inch peak, the minimum displacement $x_0(\text{min})$ would be about 5×10^{-4} centimeters rms.

It is interesting to notice that the sensitivity can approach that of the coherent systems if the maximum displacement is no greater than an optical wavelength, good optics are used, and the receiver aperture is large. In such a situation, the spatial coherence of the laser is fully utilized. Such a system is therefore not incoherent in the limit.

For large vibrations the system has many advantages and a few disadvantages. The main disadvantage is the need for careful alignment of the receiver and knife-edge. For scanning, the separate receiver and transmitter are troublesome. However, tolerance on the optical components is not severe for large maximum displacements, and other components are simple and reliable.

Coherent Spot Projection System. - The "incoherent" system above measures normal displacement of the surface. The coherent system to be described measures angular tilt of the surface in the plane determined by the transmitter and receiver axes. Figure 9 illustrates the system schematically. Two small spots are projected by high quality optics. They are separated on the surface by a distance approximately equal to a spot diameter. Then at the receiver plane there will be interference

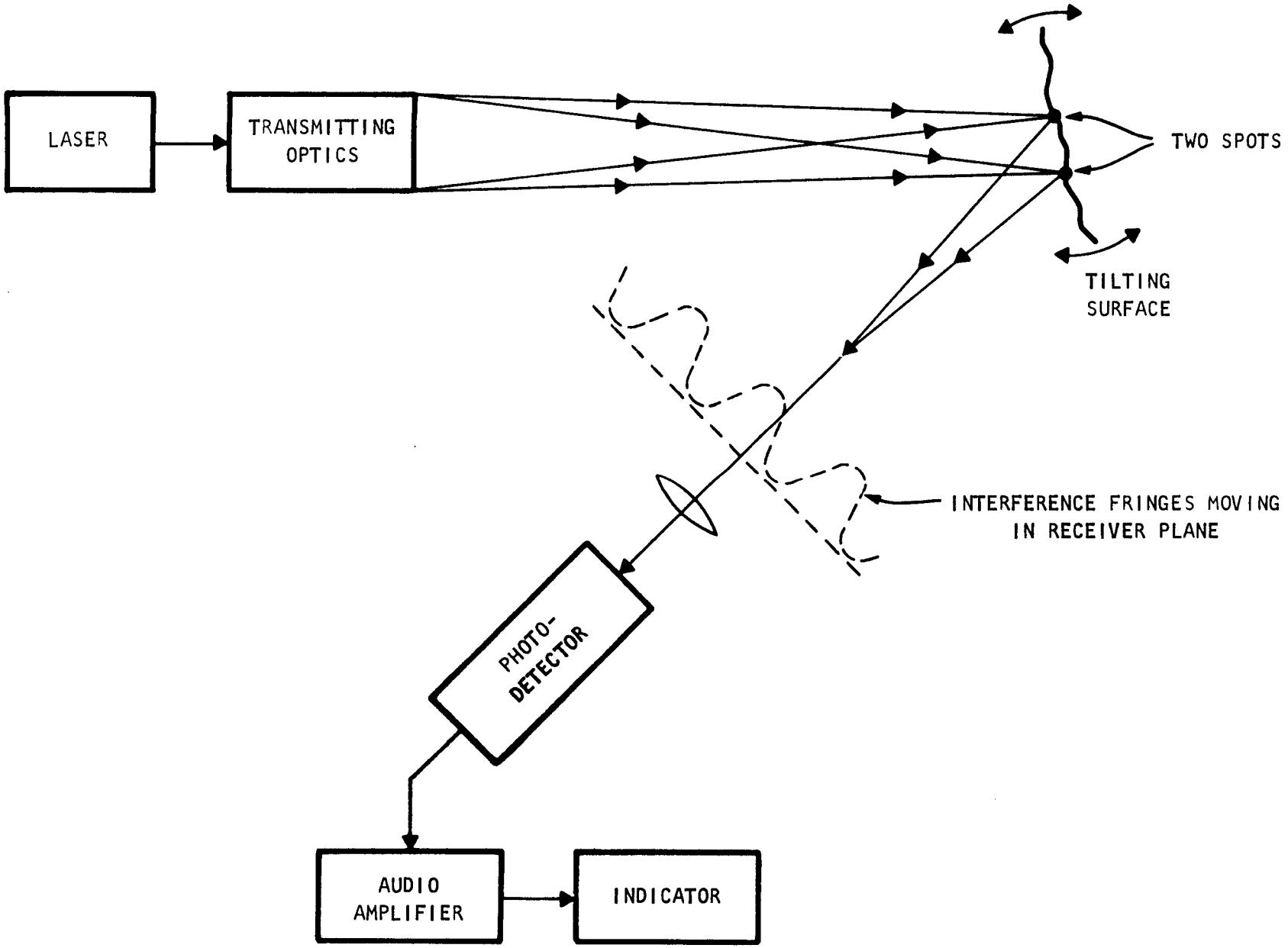

Figure 9. Coherent Spot Projection System.

fringes produced by reflected light from the two spots. If the spot separation is sufficiently small, the fringes can become large enough to fill a receiver aperture of a few inches. A tilt of the surface corresponding to a relative motion between the spots equal to 1/2 optical wave will move the fringe pattern laterally by a full spatial period. Power changes due to motion of the fringe pattern are detected in the receiver. The spot separation corresponding to a three-inch receiver at three feet is about 4×10^{-4} inches or 10^{-2} millimeters. The tilt associated with a half-wave relative motion is then approximately 30 milliradians or about 1.7 degrees.

A visual test of this method was tried in the laboratory. Two difficulties were encountered. First of all, the diffuse surface causes self-interference in the reflected light from each spot. Thus at any point in the receiver plane, the fields from the spots are likely to be far from equal. Consequently, the desired fringes have very low contrast over most of the plane, and must be detected in the presence of a large, strongly modulated background of random interference. The second problem is the inability to produce very small spots on a diffuse surface. Scattering among the rough elements near the illuminated region spreads the effective spot size considerably, thus reducing the maximum usable receiver aperture. Because of these problems and the need to keep the receiver aperture carefully positioned in the fringe pattern for linear demodulation (a condition difficult to meet if the surface must be scanned), this approach is not very promising.

Interference Displacement Mapping System

The approaches considered thus far have been quantitative, but they have required a separate measurement of excursion or tilt for each point on the moving surface in order to obtain a picture of the vibration mode of the surface as a whole. For diffusely reflecting surfaces, it is

possible to avoid most of the quantitative measurements by employing a qualitative technique for locating those areas of maximum and minimum excursion.

One possible approach for doing this is simply to use a laser to make a hologram of the surface (refs. 1, 2). The hologram reconstruction would fail to image those areas of the surface that move more than a fractional optical wavelength during the exposure. This idea was quickly rejected as impractical because the physical apparatus used in vibration testing is probably not sufficiently rigid during the many seconds of exposure to make any portion of the surface register on the hologram. Also this technique is necessarily photographic and requires slow, high resolution film.

An alternate method, which can be visual or photographic, has been suggested and tested with encouraging results. This system makes use of the random interference patterns which always appear when laser light is used to illuminate a diffuse reflector. These random "sparkle" patterns are produced by reflected waves of random phase which overlap in the region of space in front of the surface. They may be viewed by eye, often with the aid of a lens and iris diaphragm, and they can be photographed.

The important characteristic of the sparkle patterns for this application is the fact that they are correlated with the positions of the many small scatterers, or rough surface elements, that make up the diffuse reflector. If the reflector moves, so does the complex interference pattern. By viewing the pattern in front of the surface from the vicinity of the illuminating laser source, one can detect tilt of the surface as a lateral motion of the sparkle pattern. If this tilt occurs at a rate faster than the eye can follow, the motion appears as a streaking of the pattern in the direction of the tilt. What is actually indicated then is the gradient of the surface excursion in the direction of the observer.

The system for interference mapping is shown in Figure 10. The viewing lens allows the observer to focus on the interference in a particular plane. An iris is often helpful because the granularity of the pattern is always just at the diffraction limit of resolution for the viewing aperture. The imaged granularity, however, must be larger than the resolution of the human retina or the film grain to be seen. The iris diaphragm therefore makes the imaged patterns coarser so that the retina or film can view the interference conveniently. This reduces the available light and the sensitivity of the technique, however, so that a compromise would have to be made in a practical situation.

The theoretical sensitivity of this method is very good. As the surface is tilted, the angular motion of the interference patterns about the corresponding reflecting elements on the surface is twice the tilt angle. This is true because of the same phase relations which lead to the well-known law of reflection for specular surfaces in geometrical optics. For streaking to occur, the interference patterns, or granules, must move at least an amount equal to their diameter. As stated above, this diameter is determined by the viewing system. Thus the greater the distance from the surface to the patterns, and the higher the viewer resolution, the better will be the angular sensitivity. As an example, assume a viewing aperture d_1 of 6 millimeters, a viewer-to-pattern distance L_1 of one meter, and a surface-to-pattern distance L_2 of one meter. The physical diameter of the average interference granule is then given by:

$$d_2 = \frac{\lambda L_1}{d_1} = \frac{6 \times 10^{-5} \times 100}{6 \times 10^{-1}} = 10^{-2} \text{ centimeters.}$$

Then the minimum tilt angle at the surface which will cause streaking is approximately:

$$\alpha = \frac{1}{2}\frac{d_2}{L_2} = \frac{\lambda L_1}{2 d_1 L_2} = 5 \times 10^{-5} \text{ radians.}$$

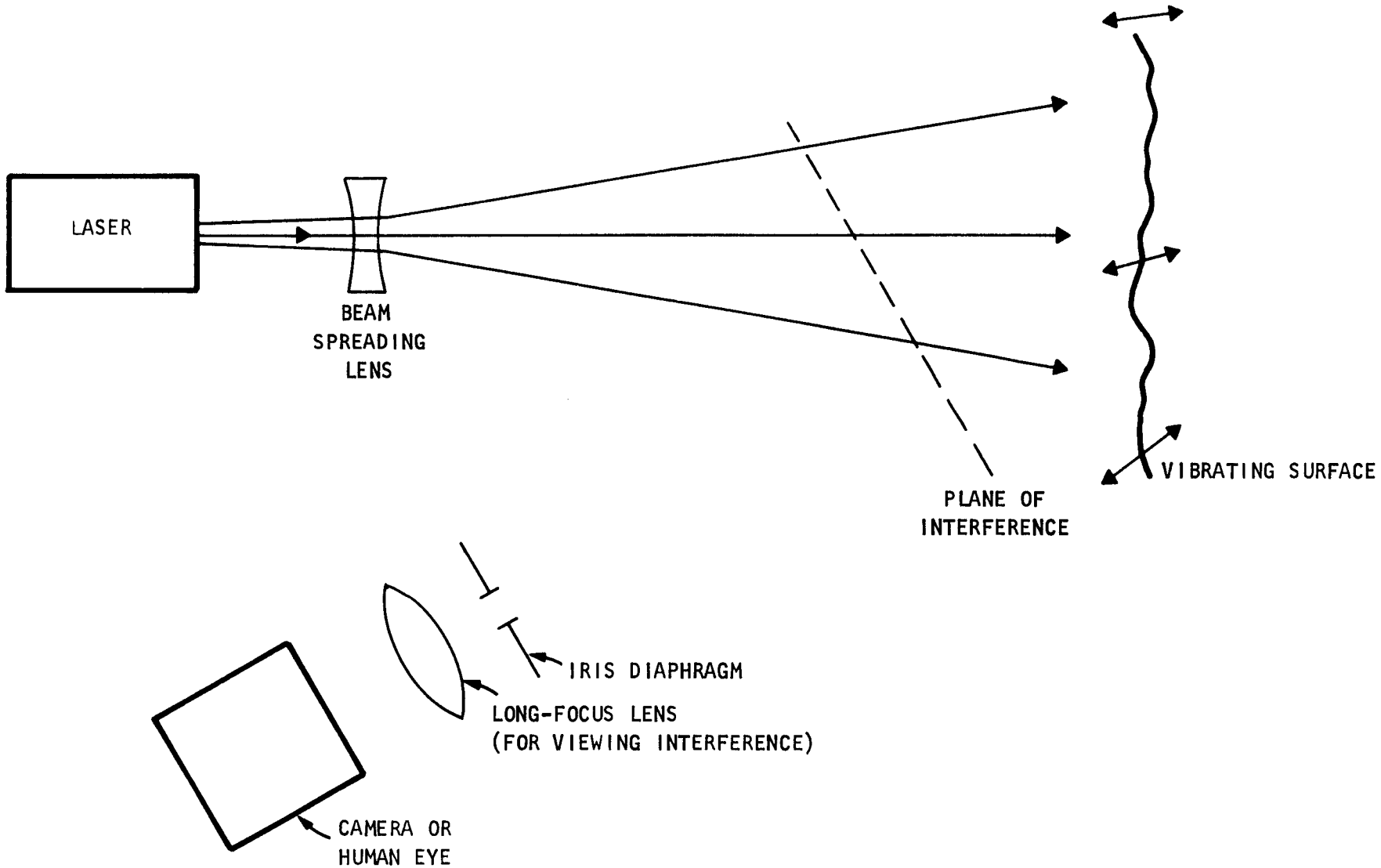

Figure 10. Interference Displacement Mapping System.

From the algebraic relations above, it is seen that the minimum tilt is about one half of the physical (diffraction-limited) angular resolution limit for a perfect lens whose aperature is equal to the iris opening d_1, provided that $L_1 = L_2$. The ratio of these distances provides a magnification factor which can enhance or reduce the sensitivity.

Visual and photographic tests of the system were made on a vibrating sheet metal surface excited by sound from a loudspeaker bolted to one face, as shown in Figures 11 and 12. The illuminating and viewing geometry was the same as in Figure 10. With the loudspeaker turned off, the interference sparkle patterns appeared as in the photograph in Figure 13. Figure 14 shows the resultant pattern obtained when the speaker was driven at 550 cps. The radial streaks indicate a displacement maximum at the center of the plate, a minimum in a circle where the frame of the loudspeaker is fastened, and some vibration at the edges. The vibration amplitude was quite small, probably of the order of 10^{-3} centimeters. The streaking was readily visible to the unaided eye several feet from the surface. The light source was a 15 milliwatt laser with lenses to spread the illuminating beam uniformly over the surface. Exposure time was 30 seconds.

The tests indicate that the mapping technique works essentially as predicted by theory. It appears to be a useful qualitative aid which may reduce the amount of data to be taken using other quantitative techniques.

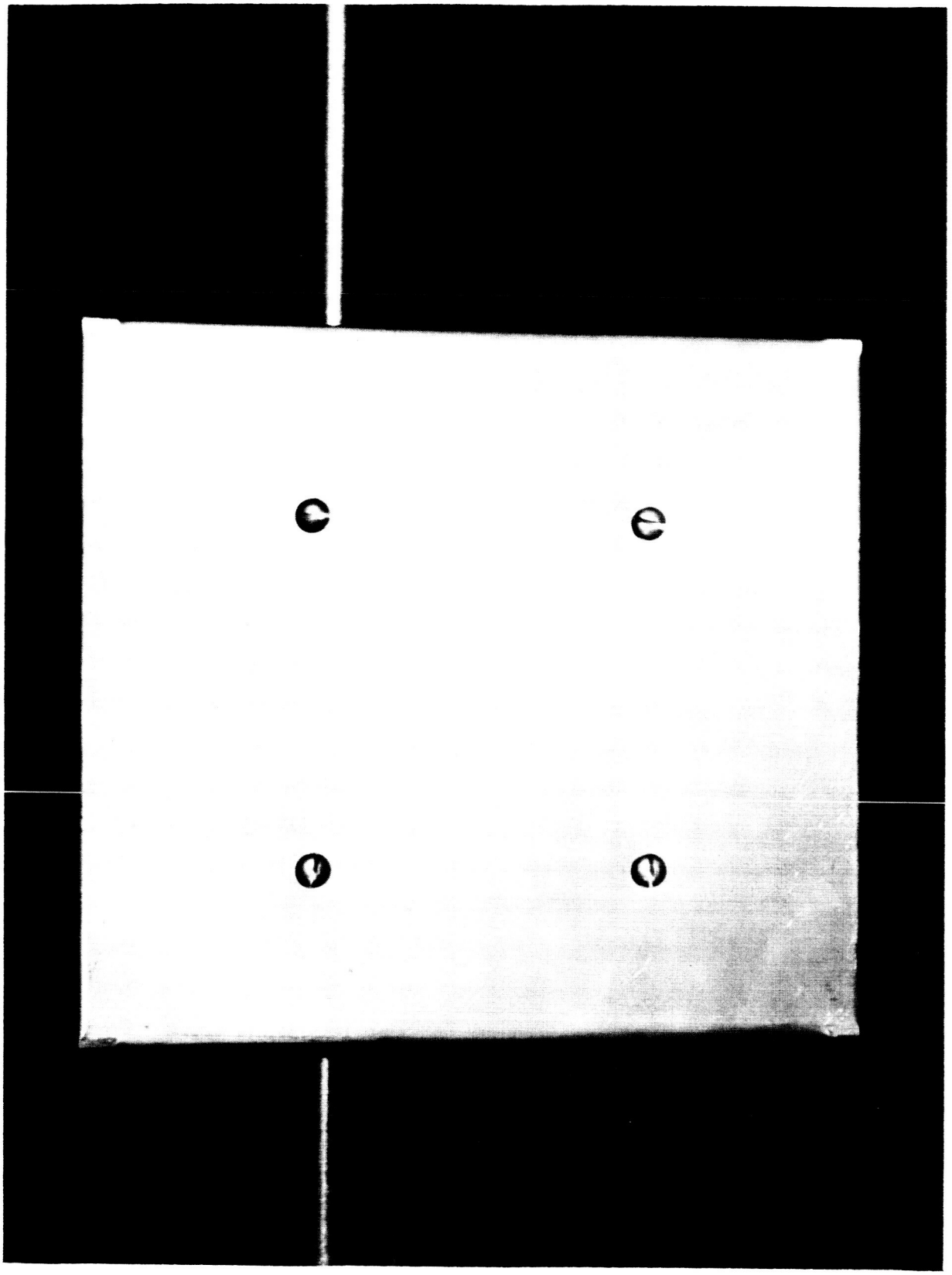

Figure 11. Vibrating Panel.
Front View.

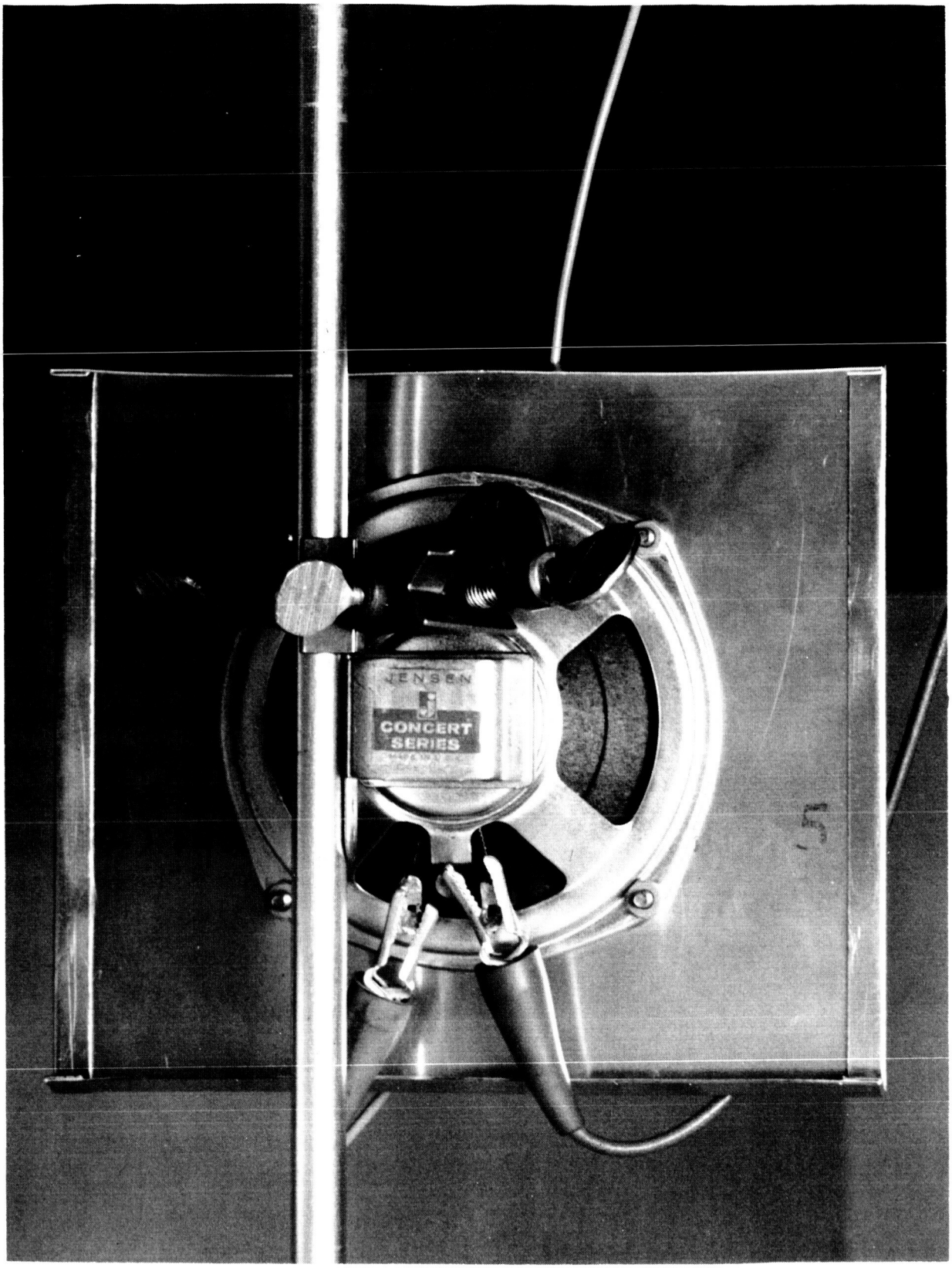

Figure 12. Vibrating Panel.
Back View.

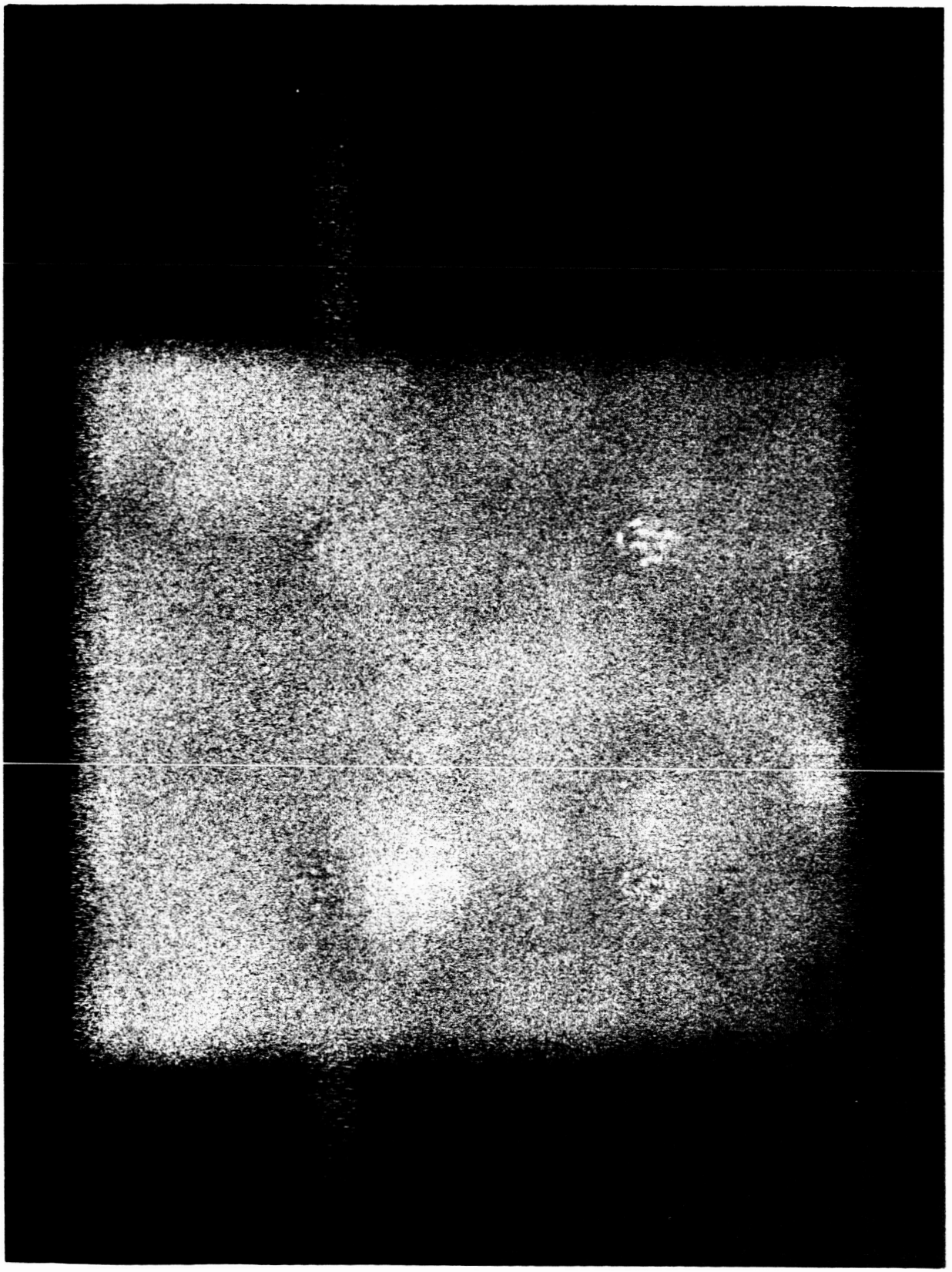

Figure 13. Interference Patterns.
Vibration Amplitude = 0.

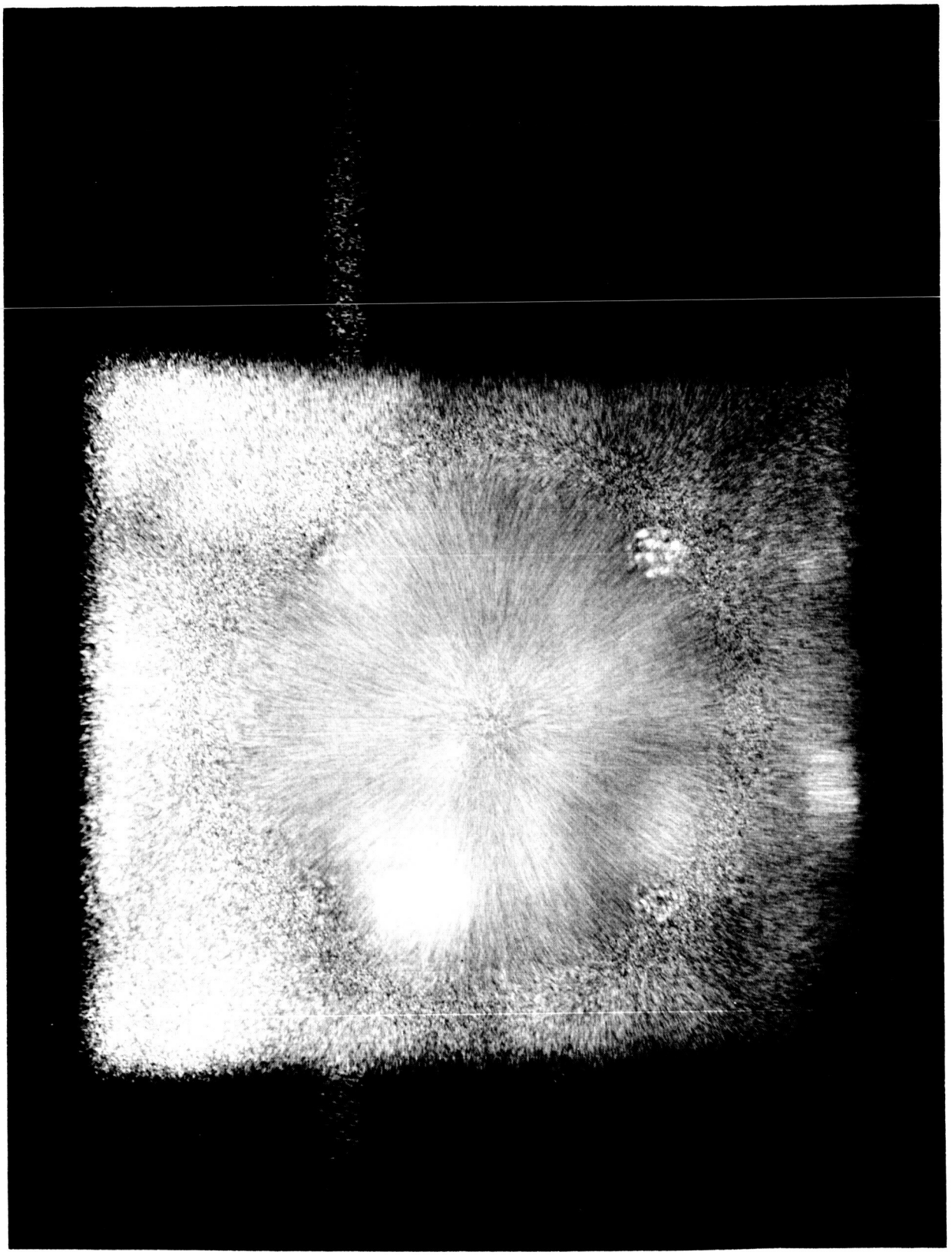

Figure 14. Interference Patterns. Vibration Amplitude Approximately 10^{-3} Centimeters.

CONCLUDING REMARKS

A variety of techniques for vibration detection and measurement have been proposed, investigated, and compared. The microwave systems have low sensitivity even for specular surfaces. The spot projection system offers some promise, but would be difficult to use in a scanning mode because of the separation of transmitter and receiver. The coherent detection systems, using one aperture for transmission and reception, should provide the best sensitivity, and will deliver that sensitivity with a laser of smaller size and lower power output. In particular, the coherent optical intermediate frequency system appears to offer very good versatility with regard to vibration waveshape, range of vibration amplitudes, and the possibility of operation in a scanning mode. In addition, the interference displacement mapping system may provide a direct visual means of locating those areas where the largest vibration occurs, thus minimizing the necessary measurements to be made with the other system.

Laboratory verification of the fundamental concepts involved with the coherent IF system and the mapping system has been demonstrated during the study. However, these first tests have been made without attempting to scan, and they have been conducted only on nearly flat vibrating sheet metal surfaces and mirrors. Before a working system can be built, more tests of the coherent system on surfaces of very general shape, and in the scanning mode, are recommended. This is necessary because the scanning of a three-dimensional object introduces time variations in the optical path that may be identical to the effects produced by vibrations. Thus it may be found that point-to-point stationary measurements are preferable to scanning.

In addition, the desirability of a hand-held detector only a few inches from the surface is a justification for further investigations

into the possibility of non-lasering narrow spectral sources such as room-temperature gallium arsenide emitters. The spectral and spatial coherence is relatively poor for these devices, but with such short distances the problems might be avoidable by making the local oscillator path in the system equal to the external path. This type of operation, in the zero order of interference, removes some coherence restrictions.

The problems posed by the design of the wideband circuitry which would be needed for the coherent system do not seem unusual or particularly difficult. However, the tests conducted thus far have been with a spectrum analyzer as the receiver. Difficulties with limiting under small-signal conditions with large input fluctuations can only be determined by construction of an experimental receiver to be used with the optical components. This would be particularly useful in evaluating the problems introduced by scanning.

In conclusion, the coherent system and the mapping system make use of the unique coherence properties of laser radiation, and probably can be developed into useful instruments for analyzing mechanical vibrations with amplitudes between a centimeter and a micron.

APPENDIX A

SYLVANIA MICROWAVE LIGHT MODULATOR

Application Note: February 1965

SYLVANIA MICROWAVE LIGHT MODULATOR

The Sylvania Microwave Light Modulator is a device capable of phase, frequency, and amplitude modulation of light at a microwave frequency. A typical application of the modulator is shown in Fig. 1. In this case, it is used as an amplitude modulator for an He-Ne gas laser, and the signal is received on a Sylvania Traveling-Wave Phototube.

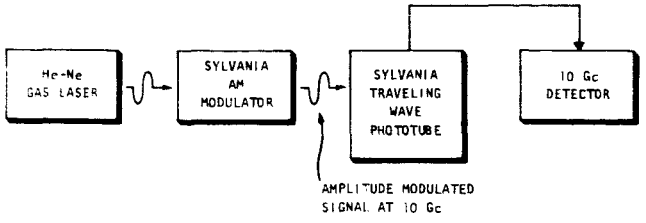

Figure 1. Typical Application of Sylvania Microwave Light Modulator.

I. General Discussion

A. Electro-Optic Effect

Microwave-modulated light may be obtained by utilizing the linear electro-optic effect in potassium dihydrogen phosphate (KDP). The heart of the Sylvania Light Modulator is a microwave cavity containing a crystal of KDP. A schematic of the microwave cavity is shown in Fig. 2. The KDP is cut in the form of a bar with its optic axis along its length.

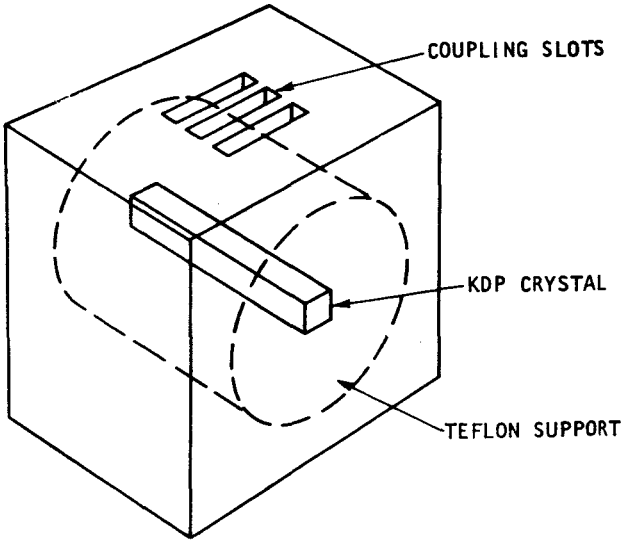

Figure 2. Sketch of Modulator Cavity.

In the absence of an applied electric field, KDP is a uniaxial crystal; and for light propagating along the optic axis of the crystal, the two principal indices of refraction will both be equal to the ordinary index of refraction, n_o. That is, light of any polarization which travels through the crystal parallel to the optic axis will experience the same index of refraction. However, an electric field applied parallel to the optic axis resolves this degeneracy in the indices of refraction, and light propagating parallel to the optic axis develops two principal indices of refraction given by

$$n_1 = n_o + kE_z$$
$$n_2 = n_o - kE_z \qquad (1)$$

where E_z denotes the magnitude of the electric field in the z-direction, and k is a constant representing the effect of the applied E field. Figure 3 is a schematic of a KDP crystal showing the directions of the electrically induced principal axes in the crystal. These axes are located at 45° to the principal cleavage planes of the crystal, and it is important to note that the position of these axes is independent of the applied electric field strength.

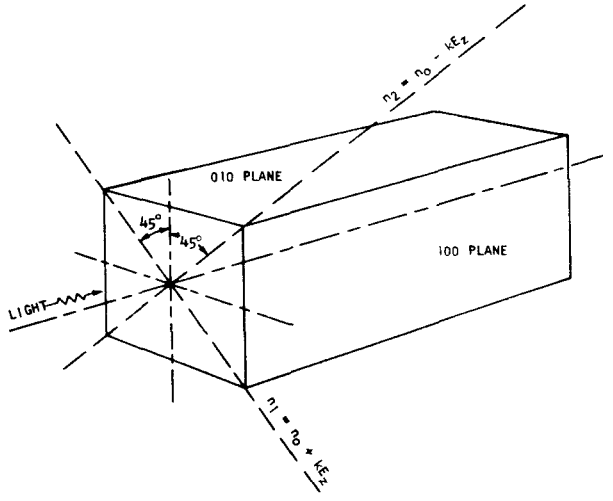

Figure 3. KDP Crystal.

B. Phase Modulation

To obtain microwave frequency- or phase-modulated light, microwave power is applied to the resonant cavity which is operated in a TM mode. A strong axial E field is developed along the optic axis and the incident light is polarized along one of the electrically induced principal axes. As the optical signal travels through the modulator, the instantaneous index of refraction that it sees is dependent on the applied electric field strength. The result is that the phase of the transmitted light is dependent on the applied electric field strength, and the light emerges from the modulator phase modulated. If the optical electric field at the input of the modulator is written as $E = E_{in}e^{jwct}$, then the output electric

field is given by

$$E_{out} = E_{in} \exp j\,[w_c t + \delta \cos \omega_m t] \qquad (2)$$

where ω_c and ω_m are the carrier and modulation frequencies, respectively. This is a phase-modulated signal with a peak phase deviation δ, and a peak instantaneous frequency deviation of $\omega_m \delta$. The peak phase deviation δ varies directly with the KDP crystal length, the applied electric field strength, the index of refraction n_o, and the electro-optic coefficient; it varies inversely with the optical wavelength. The orientation of the polarizer and crystal for this mode, designated the FM mode, is schematically depicted in Fig. 4.

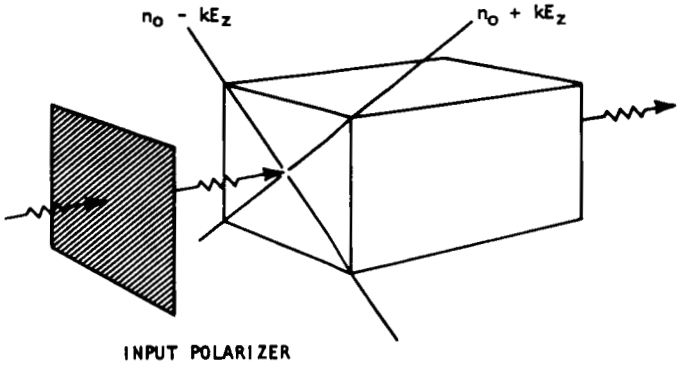

Figure 4. FM Mode of Operation.

C. Amplitude Modulation

To obtain microwave amplitude-modulated light, the microwave cavity containing the KDP crystal is combined with appropriate polarizers and retardation elements such that the incident light is divided into orthogonal components which have equal amplitude along the two electrically induced principal axes of the KDP crystal. Each component is phase modulated as it passes through the crystal, with the result that the light at the output of the crystal is polarization modulated. That is, the polarization of the light at the output of the KDP is dependent on the electric field strength that is applied to the KDP crystal. If the modulator is then followed by an appropriately oriented analyzer, the polarization modulation may be converted to amplitude modulation.

The ratio of the output intensity to the input intensity when the modulator is run in the AM position is given by

$$\frac{I_{out}}{I_{in}} = \tfrac{1}{2} + \cos\varphi\left[\frac{J_o(2\delta)}{2} + \sum_{n=1}^{\infty} (-1)^n J_{2n}(2\delta) \cos 2n\omega_m t\right] + \sin\varphi\left[\sum_{n=o}^{\infty} (-1)^{n+1} J_{2n+1}(2\delta) \cos(2n+1)\,\omega_m t\right] \qquad (3)$$

In the above expression φ is termed the bias and represents any additional retardation that is present along one of the electrically induced principal axes and not the other. By adjusting φ, the harmonic content of the intensity-modulated wave may be varied. The Sylvania Light Modulator is constructed such that φ may be conveniently adjusted to any desired value. Two types of operation are, however, particularly useful.

In the first, which we call the fundamental AM mode, the bias is set equal to $\frac{\pi}{2}$, and the output intensity thus becomes

$$\frac{I_{out}}{I_{in}} = \tfrac{1}{2} - J_1(2\delta) \cos \omega_m t + \text{odd harmonics} \qquad (4)$$

This is amplitude modulation at the fundamental frequency with the index of modulation given by

$$m = \frac{I_{ac}}{I_{dc}} = 2J_1(2\delta) \qquad (5)$$

Figure 5 is a plot of m versus δ, and it is seen that the modulator is fairly linear for modulation depths up to 100%. The $\frac{\pi}{2}$ bias is achieved by inserting a quarter-wave plate with its principal axes parallel to the electrically induced principal axes of the KDP crystal. Figure 6 represents schematically this mode of operation.

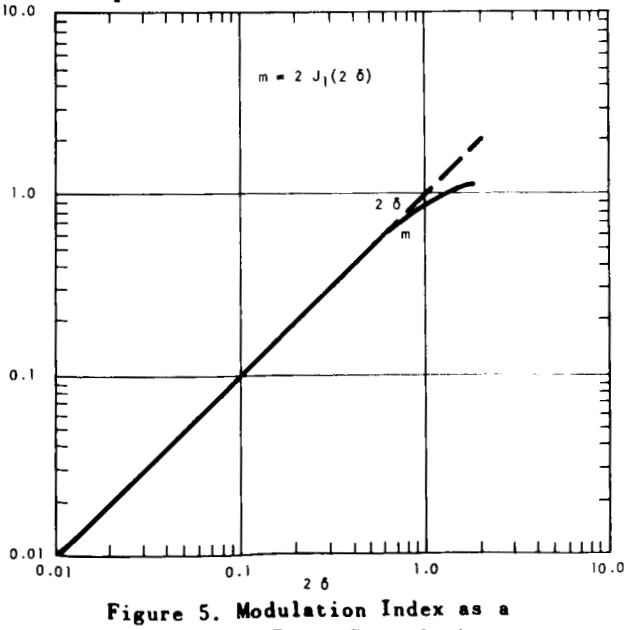

Figure 5. Modulation Index as a Function of Phase Retardation.

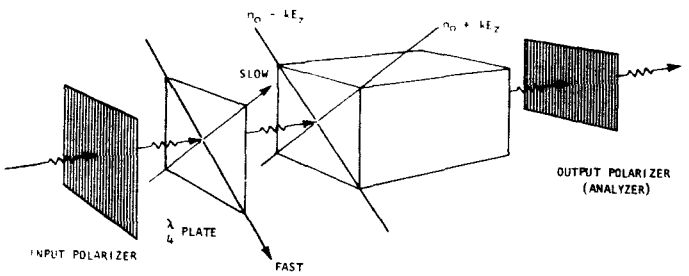

Figure 6. AM Fundamental Mode.

In the second useful mode of operation, the bias is set equal to π, and the output intensity then becomes

$$\frac{I_{out}}{I_{in}} = \frac{1}{2} - \frac{1}{2}J_0(2\delta) + \text{even harmonics} \qquad (6)$$

This mode of operation is useful since the average transmitted intensity is dependent on δ, and it thereby provides a useful method for the measurement of the modulation index. This mode may also be used to provide intensity-modulated light at higher even harmonics of the modulation frequency. In this mode, designated the AM closed mode, no quarter-wave plate is used. The orientation of the components is shown in Fig. 7.

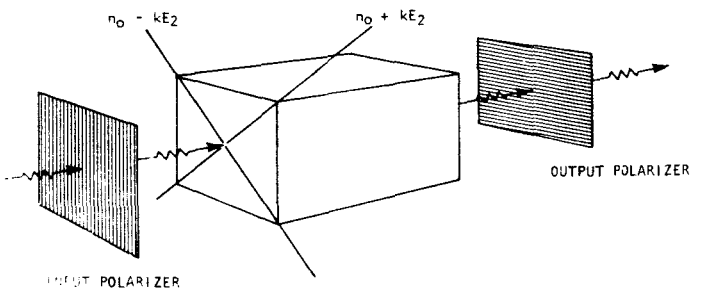

Figure 7. AM Closed Mode.

D. Single-Sideband Suppressed-Carrier Modulation

One very useful mode of operation is single-sideband suppressed-carrier optical modulation. This type of modulation finds applications in experiments requiring a microwave shift in the output frequency of the laser. Experiments in this laboratory have demonstrated that the basic modulator can be used, with slight modification, for single-sideband modulation (see ref. 15 in the bibliography). Upon request, further information will be supplied concerning this mode of operation and the adaptations necessary for using the Sylvania Microwave Light Modulator for single-sideband modulation.

II. Operating Instructions

Directions for use of the modulator divide into three main categories: (a) optical alignment of the cavity; (b) positioning and use of the quarter-wave plate and polarizers; and (c) microwave power requirements and adjustments. A method of measuring the modulation index m for amplitude modulation will also be detailed.

A. Cavity Alignment

Before attempting to align the cavity in the optical beam, the beam should be well collimated with a cross-sectional diameter of approximately one-tenth of an inch. Once this has been accomplished, the modulator cavity may be placed in the beam and aligned. One of the simplest methods for determining whether the crystal is parallel to the beam is to observe the cross and circle pattern produced when the crystal is between crossed polarizers. To do this, remove the quarter-wave plate from the modulator, position the input polarizer to 0° and the output polarizer to 90°. When the crystal is aligned correctly in this manner, the pattern of the light coming through the modulator and displayed on a screen will be similar to the one sketched in Figure 8. The modulator will be correctly positioned when the darkened center is in the position on the screen of the beam when no modulator is in the beam's path. If it is difficult to recognize this pattern, a piece of diffused glass placed in the original position of the quarter-wave plate may be used as an aid for preliminary alignment. The glass enables one to see the pattern distinctly, but it should be removed before the final alignment is set.

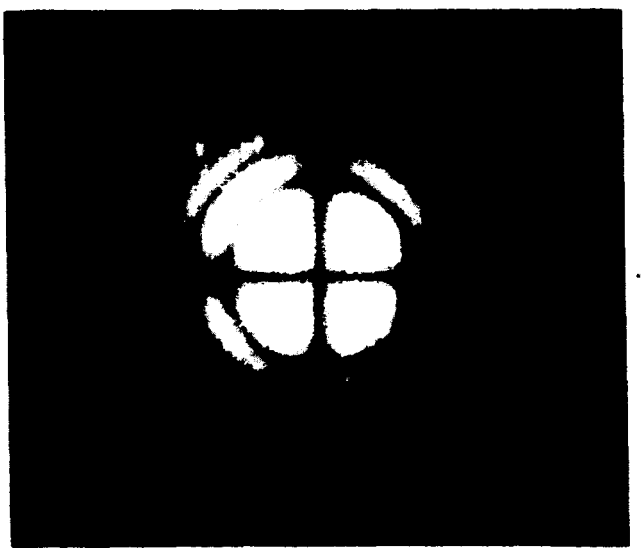

64020513

Figure 8. Cross and Circle Pattern.

B. Polarizers and Quarter-Wave Plate

The polarizers and quarter-wave plate have been

calibrated and positioned on the modulator for ease of operation in all experiments. For FM or phase modulation, the input polarizer should be set to 45°, and the quarter-wave plate and output polarizer should be removed. Amplitude modulation is accomplished by placing the input polarizer to 0°, the quarter-wave plate to 45°, and the output polarizer 0°. Removing the quarter-wave plate, adjusting the input polarizer to 0°, and adjusting the output polarizer to 90° generates the AM closed mode. It should be pointed out that although the KDP crystal will modulate light in the wavelength range from .4 microns to 1.3 microns, the quarter-wave plate is actually designed for .6328 microns. If another frequency is desired for modulation, then the appropriate quarter-wave plate will be supplied upon request.

C. Microwave considerations

Modulators are available for modulation at L, S, C, or X band. Each modulator is tested, and the resonant frequency, modulation index, and bandwidth are supplied with it. The L-and S-band modulators are supplied with coaxial outputs; the C-and X-band modulators have waveguide adaptors. It may prove convenient to use a slide-screw or stub tuner for optimum coupling to the cavity. *(See note, p.5.)*

Due to heating of the KDP crystal, the average microwave power delivered to the cavity should not exceed one watt. If a very high modulation index is desired, this may be achieved by pulsing the microwave power. The average power to the cavity should however remain below one watt although the peak power may be as large as desired. The modulation indices quoted for the modulators are obtained by applying two watts of peak power to the cavity with a 50% duty cycle, thus keeping the average power at one watt.

D. Modulation Index Measurements

One convenient method of measuring the modulation index m is the following.

1. Align the cavity optically as outlined in Section IIA.
2. With the quarter-wave plate removed, the input polarizer set at 0°, and the output polarizer at 90°, square-wave modulate the microwave power into the cavity at one kc.
3. Let the output from the modulator fall on a photomultiplier. If the output of the photomultiplier is connected to an oscilloscope, a one kc square wave should be observed. Measure the peak-to-peak value of the square wave and call this value V_1(volts).
4. Turn off the microwave power and turn the output polarizer to 0°. Then measure the change of the dc value of the output of the photomultiplier when the beam is blocked (with a piece of paper), and when it is not blocked. Call this change in dc level V_0(volts).
5. Referring to Section IC, Figure 9 is a graph comparing Equation 6 with the approximation

$$2\delta = 2\sqrt{2}\,\frac{I_{out}}{I_{in}} \qquad (7)$$

and Figure 5 compares Equation 5 with the approximation

$$m = 2\delta \qquad (8)$$

Using these approximations, then m becomes

$$m = \sqrt{\frac{8V_1}{V_0}} \qquad (9)$$

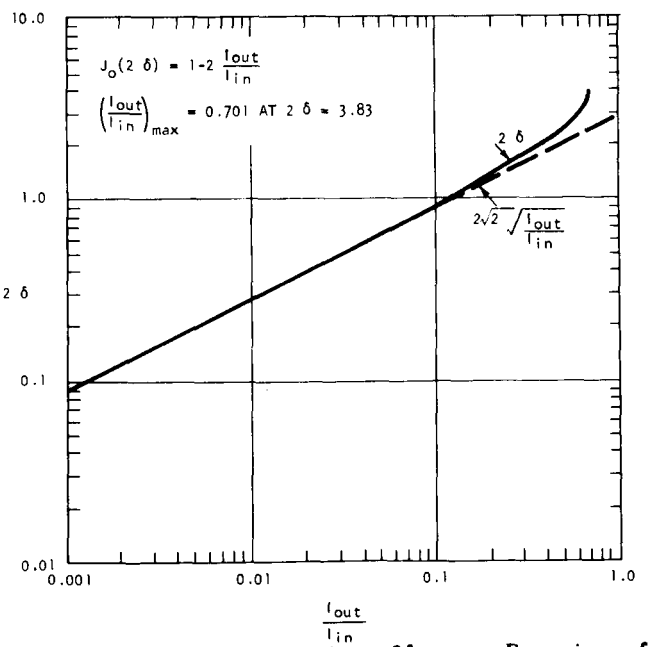

Figure 9. Phase Retardation, 2δ, as a Function of the Change in the d-c Level of the Transmitted Light.

III. Bibliography

1. Billings, B. H., "The electro-optic effect in uniaxial crystals of the type XH_2PO_4. I. Theoretical," Journal of the Optical Society of America, 39, 797, (October 1949).
2. Billings, B. H., "The electro-optic effect in uniaxial crystals of the type XH_2PO_4. II. Experimental," Journal of the Optical Society of America, 39, 802, (October 1949).

3. Blumenthal, R. H., "Design of a microwave-frequency light modulator," Proceedings of the IRE, 50, 452, (April 1962).
4. Buhrer, C. F., "Optical modulation by light bunching," Proceedings of the IEEE, 51, 1151, (August 1963).
5. Buhrer, C. F., L. R. Bloom, "Single-sideband modulation and reception of light at VHF," Proceedings of the IRE, 50, 2492, (December 1962).
6. Buhrer, C. F., L. R. Bloom, D. H. Baird, "Electro-optic light modulation with cubic crystals," Applied Optics, 2, 839, (August 1963).
7. Buhrer, C. F., V. J. Fowler, L. R. Bloom, "Single-sideband suppressed-carrier modulation of coherent light beams," Proceedings of the IRE, 50, 1827, (August 1962).
8. Carpenter, R. O'B., "The electro-optic effect in uniaxial crystals of the type XH_2PO_4. III. Measurement of Coefficients," Journal of the Optical Society of America, 40, 225, (April 1950).
9. Harris, S. E., "Demodulation of Frequency-Modulated Light," (Doctoral Dissertation), Rept. SEL-63-073 (TR No. 0576-5), Stanford Electronics Laboratories, Stanford, California, October 1963, Ch. IV.
10. Holshouser, D. F., H. Von Foerster, G. L. Clark, "Microwave modulation of light using the Kerr effect," Journal of the Optical Society of America, 51, 1360, (December 1961).
11. Kaminow, I. P., "Microwave modulation of the electro-optic effect in KH_2PO_4," Physical Review Letters, 6, 528, (May 15, 1961).
12. Kaminow, I. P., G. O. Harding, "Complex dielectric constant of KH_2PO_4 at 9.2 Gc/sec," Physical Review, 129, 1562, (February 15, 1963).
13. Mason, W. P., "Electro-optic and photoelastic effects in crystals," Bell System Technical Journal, 29, 161, (April 1950).
14. Saito, S., T. Kimura, "Microwave modulation of ruby laser light using KDP crystal," Japanese Journal of Applied Physics, 2, 658, (October 1963).
15. Targ, R., "Optical heterodyne detection of microwave-modulated light," Proceedings of the IEEE, (to be published in March 1964).

NOTE: The microwave resonant frequency is determined individually for each modulator, and is noted in the data shipped with each unit. The S-band unit will be resonant at about 2.5 Gc; the X-band unit at about 10.7 Gc. The cavity is not arranged for tuning, its frequency being determined by its dimensions and by the properties of the Teflon and KDP contained within the cavity.

APPENDIX B

FM OSCILLATION OF THE HE-NE LASER

S. E. Harris and Russell Targ

Published in Applied Physics Letters,
Vol. 5, No. 10, 15 November 1964, pp. 202-204.

FM OSCILLATION OF THE He-Ne LASER[1]

S. E. Harris
Consultant to Sylvania Electronic Systems
Mountain View, California and
Department of Electrical Engineering
Stanford University, California

Russell Targ
Electronic Defense Laboratories
Sylvania Electronic Systems
Mountain View, California

(Received 25 September 1964)

(internal phase perturbation; interferometry; KDP crystal; E)

We report the operation of a He-Ne laser in a manner such that all of the laser modes oscillate with FM phases and nearly Bessel function amplitudes, thereby comprising the sidebands of a frequency-modulated signal. The resulting laser oscillation frequency is, in effect, swept over the entire Doppler line-width at a sweep frequency which is approximately that of the axial mode spacing. This type of FM oscillation is induced by an intra-cavity phase perturbation which is driven at a frequency which is approximately but not exactly the axial mode spacing. Experimental evidence supporting the hypothesis of an essentially pure FM oscillation is as follows:

1. The suppression of all observable laser "beat notes" by at least 25 dB, as compared to their value in the absence of the phase perturbation. A 5%

increase in laser power was observed coincident with this suppression.

2. The observation of a scanning interferometer showing the laser modes to possess approximately Bessel function amplitudes, appropriate to the spectral components of a pure FM signal.

3. Direct demodulation of the resultant FM signal using both a Michelson interferometer and a birefringent discriminator.[2]

The laser was a Spectra-Physics Model 116 operated at 6328 Å, with an external mirror spacing corresponding to an axial mode interval ($c/2L$) of 100.5 Mc/sec. The phase perturbation was obtained via the electro-optic effect in a 1-cm long KH_2PO_4 (KDP) crystal which was anti-reflection coated and situated in a 100-Mc/sec tuned circuit inside the laser cavity. The KDP crystal was oriented with its optic axis parallel to the axis of the laser tube, and with one of its electrically-induced principal axes parallel to the direction of the laser polarization. A KDP crystal in this orientation introduces a pure phase perturbation and ideally should introduce no time-varying loss into the laser cavity. An rf input power of 2 W produced a single-pass phase retardation δ of about 0.06 rad at the optical frequency.

Of particular interest was that FM laser oscillation was not obtained when the KDP modulator was tuned exactly to the frequency of the axial mode spacing. In this case, the laser beat notes as observed on an rf spectrum analyzer were stabilized and enhanced, and appeared similar to those described by Hargrove and others,[3] and DiDomenico[4] in their papers on AM phase locking.

When the modulation frequency is detuned from the $c/2L$ frequency, then at a δ of 0.05, a frequency change of 250 kc/sec to either side produces an abrupt quenching of all of the original laser beat notes, with a coincident increase of 5% in the total laser oscillation power. This removes the possibility that the quenching of the axial mode beats is caused by some form of increased optical loss. After quenching of the original axial beat notes, a small amount of rf beat power may be observed at harmonics of the modulation frequency. At the second and third harmonics, this power level was 25 dB below that of the original beat amplitude. At the fundamental and fourth harmonics, this level was at least 15 dB below that of the original signal. Measurements at the latter two frequencies were limited by a residual AM light signal and poor photomultiplier sensitivity, respectively.

In order to directly verify the presence of an FM signal, the output of the FM laser was passed through an optical discriminator (Michelson interferometer) with a path length difference of 30 cm. The interferometer was followed by a photomultiplier and rf detector. With both arms of the interferometer open, a strong signal at the modulation frequency was observed with a 15-dB signal-to-noise ratio. If either arm of the interferometer was blocked, this signal completely disappeared.

The most interesting and perhaps startling results of our experiments were obtained by direct observation of the laser mode amplitudes with a Spectra-Physics scanning interferometer. In the absence of modulation, the laser modes appear as in Fig. 1*a*. As the modulation depth is increased, the central mode amplitude begins to fall, and the first pair of sidebands increase. At still larger δ's, the second and third pair of sidebands achieve significant amplitudes, and there is a diffusion of power toward the wings of the Doppler line. Examination shows the modes to have approximately Bessel function amplitudes, which are not determined by independent saturation of the Doppler line, as might have been expected. Figures 1*a* through 1*f* are captioned in terms of both the depth of the single-pass modulation δ, and also in terms of the depth of the frequency modulation on the output signal of the FM oscillator. This latter modulation depth is denoted by Γ, and from the "varying frequency" viewpoint of frequency modulation, it is the ratio of the peak frequency deviation to the modulation frequency. The ratio of Γ/δ, that is, the ratio by which the modulation process is enhanced by the presence of the cavity and active media, is ~ 40. Alternate measurements of Γ were made using the Michelson interferometer, and similar results were obtained. Our highest measured Γ was ~ 6, which at a modulation frequency of 100 Mc/sec corresponds to a peak-to-peak frequency swing of 1200 Mc/sec.

The process appears to be a regenerative parametric oscillation, with a resultant quenching of the original laser modes; as opposed to a phase locking process which has been considered by Hargrove and others,[3] and DiDomenico.[4] FM lasers may make possible many spectroscopic and communication applications which otherwise would have required single-mode lasers, with their correspondingly lower power.

To our knowledge, this type of FM laser was first

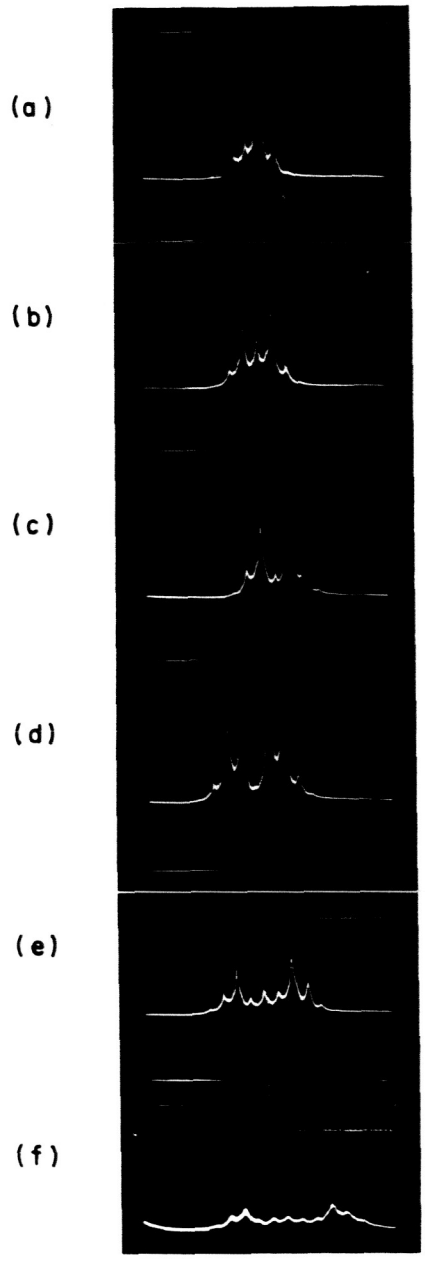

Fig. 1 Laser mode amplitudes versus optical frequency for variable modulation depth.

(*a*) $\delta = 0$ $\Gamma = 0$
(*b*) $\delta = .045$ $\Gamma \sim 2$
(*c*) $\delta = .063$ $\Gamma \sim 2.6$
(*d*) $\delta = .069$ $\Gamma \sim 2.8$
(*e*) $\delta = .072$ $\Gamma \sim 3$
(*f*) $\delta = .088$ $\Gamma \sim 4.5$

proposed by Harris in October 1963 at Stanford University under Contract AF 33(657)-11144. The problem of phase perturbations in a passive resonant cavity has been considered analytically by Gordon and Rigden.[5] The effect of phase perturbations in an active cavity has been studied by Yariv.[6,7] We greatly appreciate the encouragement and support provided by B. J. McMurtry of Sylvania and A. E. Siegman of Stanford. We acknowledge the expert technical assistance of L. E. Wilson, and thank Spectra-Physics for lending us the scanning Fabry-Perot interferometer used in these experiments.

[1]This work was partially supported by Contract AF 33(615)-1938 from the Laser Technology Laboratory of the U. S. Air Force at Wright-Patterson Air Force Base, Ohio.

[2]S. E. Harris, *Appl. Phys. Letters* **2**, 47 (1963).

[3]L. E. Hargrove, R. L. Fork, and M. A. Pollack, *Appl. Phys. Letters* **5**, 4 (1964).

[4]M. J. DiDomenico Jr., *J. Appl. Phys.* (to be published in Oct. 1964).

[5]E. I. Gordon and J. D. Rigden, *Bell System Tech. J.* **XLII**, 1, 155 (1963).

[6]A. Yariv, *Proc. IEEE* **52**, 6, 719 (1964).

[7]A. Yariv, Seminar at Stanford University and private communications.

APPENDIX C

GENERATION OF SINGLE-FREQUENCY LIGHT USING THE FM LASER

G. A. Massey, M. Kenneth Oshman, and Russell Targ

Published in Applied Physics Letters,
Vol. 6, No. 1, 1 January 1965, pp. 10-11.

GENERATION OF SINGLE-FREQUENCY LIGHT USING THE FM LASER[1]

(internal phase perturbation; E)

G. A. Massey, M. Kenneth Oshman, and Russell Targ
Electronic Defense Laboratories, Sylvania Electronic Systems
Mountain View, California
(Received 13 November 1964)

We report a technique for producing essentially single-frequency light from the entire output of a high-power multi-mode laser, without suffering the loss of power inherent in conventional approaches involving the suppression of modes. We make use of a laser in which an intracavity phase perturbation has been utilized to create an array of laser modes having the phases and amplitudes appropriate to the sidebands of a frequency-modulated (FM) signal. Such a laser has been demonstrated by Harris and Targ[2] and has been analyzed by Harris and McDuff.[3] The output of the FM laser is then passed through an external phase modulator driven 180° out of phase and with the same peak optical phase deviation as the output of the FM laser. Whereas the output from the FM laser was made up of a large number of optical frequencies, the light leaving the external modulator is in principle now a monochromatic signal.

The light output of such a laser closely approximates an FM signal and can be described as:

$$E = E_0 \cos (\omega_c t + \Gamma \sin \omega_m t) ,$$

where E_0 is the peak amplitude of the optical field, ω_c is the center frequency of the optical output spectrum, ω_m is the modulation frequency, and Γ is the peak phase deviation of the FM oscillation. If this FM signal is passed through a second phase modulator driven at the same frequency as the internal modulator, the resulting optical signal will be:

$$E' = E_0 \cos [\omega_c t + \Gamma \sin \omega_m t + \Gamma' \sin (\omega_m t + \theta)] ,$$

where Γ' is the maximum phase deviation and θ is the phase of the second modulator. If Γ' is made equal to Γ and θ equals $(2n + 1)\pi$ radians, where n is an integer, then E' becomes simply $E_0 \cos \omega_c t$ and the signal is monochromatic. If the relative phase θ is not properly set, then the signal may have FM deviations up to twice that of the FM laser.

The results of the preliminary experiments are in substantial agreement with this analysis. The experimental system is shown schematically in

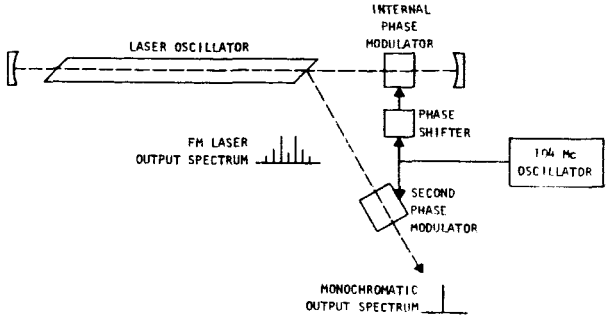

Fig. 1. Block diagram of "super-mode" laser, showing FM laser with external phase modulator.

Fig. 1. The frequency-modulated He-Ne laser was operated at 6328 Å. The laser contained a KH_2PO_4 (KDP) phase modulator in the cavity as described by Harris and Targ. As in the first FM experiments, high-reflectivity mirrors were used, with the result that substantially more light was reflected from the Brewster angle windows than was transmitted through the laser mirrors. Both outputs were FM signals, but because of its greater amplitude, the Brewster angle output was used in these experiments. The frequency difference between adjacent FM modes or "sidebands" was 104 Mc, and the output power was 100 μW.

The second, or external, modulator contained 8 cm of KDP with the applied electric field along the crystal optic axis and at right angles to the path of the light. The crystal orientation was such that the light was polarized parallel to one of the induced electro-optic axes; thus pure phase modulation was produced. Mirrors were used to reflect the light through the modulator three times. The phase shift of the modulation during transit in this device was approximately 1 radian.

Figure 2 shows the spectral content of the optical signals as photographed from oscilloscope traces made with a scanning Fabry-Perot interferometer. Figure 2*a* shows the output of the laser, free running in several frequency modes, with both modulators turned off. Figure 2*b* shows the output with the internal phase modulator energized; this

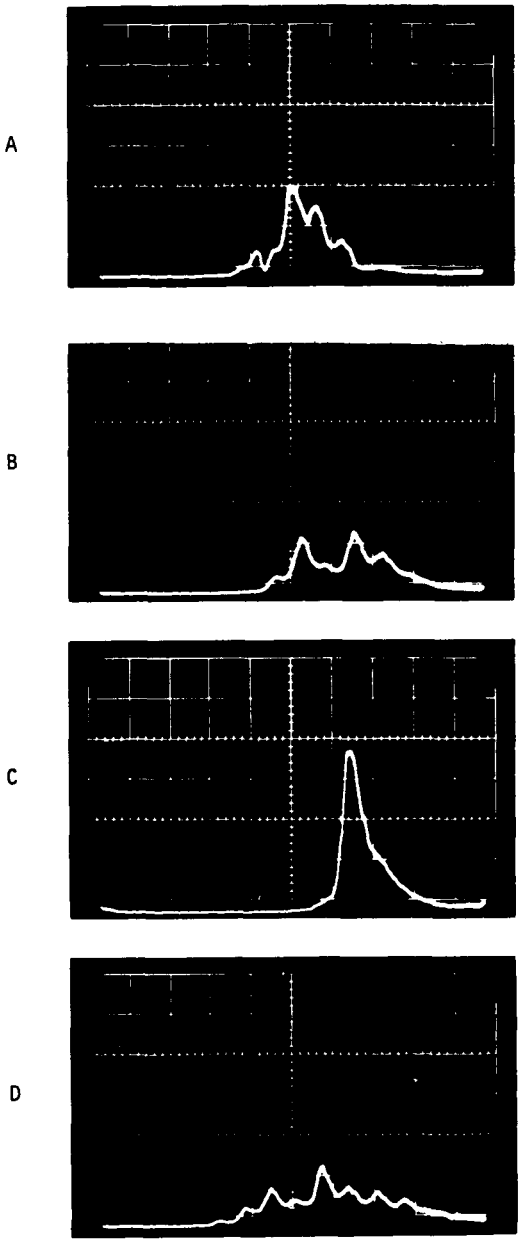

Fig. 2. Spectral composition of laser output, showing relative amplitudes. (*a*) Multi-mode laser free running. (*b*) FM laser with $\Gamma = 2$. (*c*) Output with both modulators turned on. (*d*) Output of the external modulator, $\Gamma' = 2$, with free-running laser input (no internal FM).

output closely approximates a frequency-modulated wave with Γ about 2. Figure 2*c* shows the output obtained with both modulators turned on, and with the relative phases and deviations adjusted as described above. Within the limits of error imposed by the 100-Mc resolution of the scanning interferometer, the energy of all the original modes had been converted to a single frequency or "super-mode." This condition was found to be stable with time, with only slight amplitude changes occurring in the output. The power input to the external modulator was approximately 30 W during the 1-msec interval of the Fabry-Perot scan.

The internal phase modulator converts the free-running laser from an ensemble of independent modes with random phases into an ensemble of coherent FM sidebands. This coherence is essential, if the light output is to be subsequently demodulated by the external phase modulator. If light from the free-running laser is passed through the external modulator, the result is as shown in Fig. 2*d*. This is neither a monochromatic signal nor purely frequency-modulated light, since temporal coherence was not established among the various laser modes. Pulsed excitation of the external modulator was used in this demonstration to avoid heating the KDP crystal. A variety of methods are at hand to permit operation on a cw basis. These include: use of more electro-optic material in the modulator, refinement of the multiple-pass technique, or the availability of a superior electro-optic material. It should be noted here that the single-frequency "super-mode" technique is by no means limited to gas lasers and may, in fact, find particular utility in high-gain solid-state lasers having great numbers of axial modes.

We thank Spectra-Physics Inc. for the use of the scanning Fabry-Perot interferometer.

[1]This work was partially supported by Contract AF 33(615)-1938 from the Laser Technology Laboratory of the U.S. Air Force at Wright-Patterson Air Force Base, Ohio.

[2]S. E. Harris and Russell Targ, *Appl. Phys. Letters* **5**, 202 (1964).

[3]S. E. Harris and O. P. McDuff, *Appl. Phys. Letters* **5**, 205 (1964).

REFERENCES

1. Powell, R. L.; and Stetson, K. A.: Interferometric Vibration Analysis by Wavefront Reconstruction. J. Opt. Soc. Am., vol. 55, no. 12, Dec. 1965, pp. 1593-1598.

2. Stetson, K. A.; and Powell, R. L.: Interferometric Hologram Evaluation and Real-Time Vibration Analysis of Diffuse Objects. J. Opt. Soc. Am., vol. 55, no. 12, Dec. 1965, pp. 1694-1695.

National Aeronautics and Space Administration
STUDY OF VIBRATION MEASUREMENT BY LASER METHODS.
Gail A. Massey. January 1966.

Several methods for using laser radiation to detect and measure structural vibrations were investigated. Microwave modulation on the optical carrier, coherent optical detection, and various geometrical and interference methods were analyzed and tested experimentally. Coherent detection appears to offer the greatest sensitivity and dynamic range, while the microwave systems show the lowest sensitivity. Displacement amplitudes from one-fourth inch peak down to one micron or less should be measurable using coherent detection. An interference technique for location of areas of greatest and least displacement was developed.